ERS-2 Wind Scatterometer Cyclic Report

from 24th November 2003 to 29th December 2003
Cycle 90

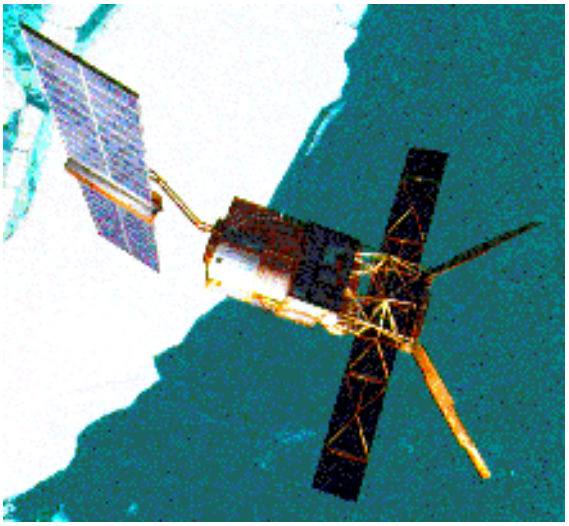

Prepared by:	PCS team	ESRIN EOP-GOQ
Inputs from:	F. Aidt	ESTEC TOS-EMS
	H. Hersbach	ECMWF

Issue:	1.0
Reference:	ERSE-SPPA-EOPG-TN-04-0001
Date of issue:	29th January 2004
Status:	Approved
Document type:	Technical Note
Approved by:	P. Lecomte

Distribution List

(Summary only via e-mail)

ESTEC	M. Canela	EOP-PEL
	E. Attema	EOP-SMS
	M. Drinkwater	EOP-SMO
	F. Aidt	TOS-EMS
	B. Gelsthorpe	EOP-PTR
	R. Zobl	EOP-P
	K. van't Klooster	TOS-EEA
ESOC	F. Bosquillon de Frescheville	TOS-OFE
	L. Stefanov	TOS-OF
ESRIN	M. Albani	EOP-GO
	P. Lecomte	EOP-GOQ
	V. Beruti	EOP-GOF
	S. Jutz	EOP-GOU
	W. Lengert	EOP-GM
	G. Kohlhammer	EOP-G
	M. Onnestam	EOP-GOC
	G. Emiliani	EOP-GOQ-PCS

L.A. Breivik	DNMI
P. Snoeij	DUT
J. Heidbreder	DORNIER
L. Isaksen, H. Hersbach	ECMWF
J. Kerkman, J. Figa	EUMETSAT
V. Wismann	IFARS
R. Ezraty	IFREMER
R.S. Dunbar	JPL
A. Stoffelen, T. Driessenaar	KNMI
G. Legg, P. Chang	NOAA/NESDIS
W. Gemmill	NOAA/NWS
J. Hawkins	NRL
D. Offiler, R. Graham, C.A. Parrette	UK-MET Office
F. Courtier, H. Roquet	Meteo-France
C. Scupniewicz	FNMOC
R.A. Brown	University of Washington
J. Boutin	LODYC/UPMC
M.A. Messeh	University of Sheffield

This report is available on PCS web:
http://earth.esa.int/pcs/ers/scatt/reports/pcs_cyclic/

1.0 Introduction and summary

The document includes a summary of the daily quality control made within the PCS and various sections describing the results of the investigations and studies of "open-problems" related to the Scatterometer. In each section results are shown from the beginning of the mission in order to see the evolution and to outline possible "seasonal" effects. An explanation for the major events which have impacted the performance since launch is given, and comments about the recent events which occurred during the last cycle are included.

This report covers the period from 24th November 2003 to 29th December 2003 (cycle 90) and includes the results of the monitoring activity performed by ESRIN and ECMWF.

Since this is the first report issued after a black-out period of roughly 9 months the following mission summary list contains also some important events occurred during the last months. Scatterometer cyclic report from cycle 82 to cycle 89 will be available in a near future.

Mission events

- On 28th February 2003 (cycle 82) the Scatterometer receiver gain was increased by 3 dB to improve the usage of the on-board ADC converter.
- Since July 16th 2003 the ERS-2 Low Rate mission is only continued within the visibility of the ESA ground stations covering: Europe, North Atlantic, the Arctic and western North America. The reason of that limited coverage was the failure of both on-board tape recorders.
- Since 21st August 2003 the new Scatterometer Attitude Corrected Algorithm (ESACA) is operational in all ESA ground station and Scatterometer winds are redistributed world-wide to the user community. That new processor is able to compensate for the effects of no intelligible platform yaw error angle on the received signal and to produce calibrated Scatterometer measurements. Backlog data will be re-processed with that new algorithm in order to fill the Scatterometer data gap (January 2001 - August 2003).
- In order to maximize the data coverage of the regional mission, since September 7th 2003 the ground stations in Maspalomas, Gatineau and Prince Albert are acquiring and processing data for all the ERS-2 satellite passes within the station visibility (apart from passes for which other satellites have an higher priority).
- To further increase the wind coverage of the North Atlantic area, since December 8th, 2003 is operative a new ground Station in West Freugh (UK) and data from this new station are available to the user since mid January 2004. Due to its location, the West Freugh acquisitions have some overlap with those from three other ESA stations, Kiruna, Gatineau or Maspalomas. The station overlap depends on the relative orbit of the satellite. Consequentially, overlapping wind scatterometer LBR data may be included in two products. Since the two products are generated at different ground stations the overlap may not be completely precise, with a displacement up to 12 Km and slight differences in the wind data itself.
- The ERS-2 satellite was piloted in ZGM throughout the cycle 90.
- During the cycle 90 the AMI instrument was operated in wind-wave mode along all orbits and the short term yaw control activity was carried out following the nominal plan.
- During cycle 90 ESACA processor worked nominally without faults.

- On 25th November 2003 was performed a touch-up manoeuvre at 22:46 UTCT and on 26th November 2003 were performed 2 touch-up manoeuvres at 00:27 and 16:00 UTCT. As expected data acquired during the manoeuvres was strong degraded and this fact explains the low quality in the winds reported by ECMWF on that day.
- No data was disseminated for the 6-hourly batch centered around 06 UTC 03 December 2003 (orbits from 45062 to 45065). Raw data are archived and available for re-processing.
- The AMI instrument was unavailable on 13th December 2003 from 14:30 to 14:54 UTCT for a payload re-synchronization after an anomaly occurred on the Radar Altimeter.

Yaw performance

- The yaw monitoring is now based on the new output of ESACA processor that is able to generate a dedicated auxiliary product (Helpful Esa Yaw - HEY) with a precise yaw estimation.
- The result of the yaw monitoring for cycle 90 is a mean yaw error angle within the nominal range (+/- 2 degrees) for most of the orbit. On 25 and 26 November 2003 some orbits shows a bad quality due to a series of orbit manoeuvres.
- Details regarding the yaw estimation and the yaw information stored in the UWI and BUFR data are given in chapter 5.

Calibration performance

- Calibration data from Transponder are regularly acquired and archived for re-processing. The CALPROC processor is not able to produce accurate gain constant with the actual degraded satellite attitude. For that reason ESRIN will initiate the TOSCA (Tool for Scatterometer CAlibration) project to re-design the calibration processor and re-compute valid gain constants coefficients.
- Due to the regional mission scenario the calibration performances over the Brazilian rain forest are not available because that area is not covered by the ESA ground station. The chance to install a new station to cover the calibration site is under investigation as well as the possibility to use stable ice area in Greenland to monitor the instrument calibration.
- The Ocean Calibration monitoring is still performed by ECMWF. The average sigma0 bias levels for cycle 90 were nearly unchanged (compared to cycle 89). Largest differences were observed at the near range descending tracks where levels have become 0.1 dB less negative. The situation is slightly better than that for nominal data in 2000 (see the ECMWEF cyclic reports for cycle 48 to 59). The dependency of the bias as function of incidence angle is small, and the tendency of being somewhat more negative at the far range has been suppressed. In fact, now levels are most negative in the near range. Internode differences are slightly smaller than for the nominal period. Bias levels are in between 0.0 and -0.5 dB. The data volume of ascending and descending tracks are similar.

Instrument performance

- During the cycle 90 the mean power decrease has been 0.13 dB per cycle.This value confirms the trend detected since the beginning of the mission.
- The noise power level was within the nominal value after the received gain increase occurred on February 2003. The daily average value is around 1.7 ADC unit for the Fore and Aft beam and it is not measurable for the Mid beam.

- The Doppler compensation performances were stable during the cycle 90 and that fact indicates the effectiveness of ESACA processor to compensate for satellite attitude changes. The CoG of the compensated spectrum is very close to zero and its standard deviation was around 1600 Hz for the Fore and Aft antenna and around 2700 Hz for the Mid antenna.

Product performance

- During cycle 90, data was received between 21:01 UTC 24 November and 19:46 UTC 29 December 2003. No data was received for the 6-hourly batch centered around 06 UTC 03 December 2003 (fast delivery dissemination problem for orbits from 45062 to 45065. Raw data was archived and available for re-processing). Due to an internal software problem at ECMWF, data was not available for the period between 18 UTC 08 December and 06 UTC 12 December 2003.
- Currently the performances of ESACA winds are affected by Land contamination. Around costal zones many Sea nodes have a strong contribution of Land backscattering and the retrieved wind is not correct. An optimization of the Land/Sea flag in the ground processing is under investigation.
- The wind statistics computed by PCS on the fast delivered winds are affected by Land and Ice contamination and for that reason the values of the wind speed bias and standard deviation are higher than nominal. With the global mission scenario that effect was present but it was negligible due to the large amount of data used to compute the statistics. A more refined Land mask used in the ground segment and the introduction of an Ice detection algorithm will improve the quality of the wind monitoring statistics.
- Quantitative performances of ESACA winds without Land and Ice contamination are summarized in the next bullet. In that case ECMWF removes from its analysis the wind nodes affected by Land and Ice contamination._RE As reported by ECMWF the performances of ESACA winds are similar to the ones obtained in the nominal YSM phase.
- Compared to cycle 89, the agreement with ECMWF first-guess (FGAT) fields was somewhat worse. Although relative bias levels have been slightly reduced (from -0.55 m/s to -0.51 m/s), scatter has increased (from 1.59 m/s to 1.65 m/s). One should note, however, that due to the lack of global coverage, this trend is likely to be a result of seasonal variations. The quality of the UWI wind direction has improved. After the negative trend observed for cycle 89, performance is back on the level of cycle 88. The quality of de-aliased CMOD4 winds (that did not show a degradation for cycle 89) remained the same. Compared to nominal data in 2000, both backscatter and wind speed bias levels are somewhat more optimal. Internode and inter-beam dependent trends were found to be similar to the old situation. Standard deviations of wind speed are less optimal to those for 2000. A fair comparison, however, cannot be made due to large differences in data coverage.
- The ERS-2 scatterometer data was not used in the 4D-Var data assimilation system at ECMWF. However, it is being processed passively in the operational suite and assimilated actively (on the basis of CMOD5) in the experimental suite that is scheduled to become operational within a few months.

2.0 Calibration Performances

The calibration performances are estimated using three types of target: a man made target (the transponder) and two natural targets (the rain forest and the ocean). This approach allow us to design the correct calibration using a punctual but accurate information from transponders and an extended but noisy information from rain forest and ocean for which the main component of the variance comes from the geophysical evolution of the natural target and from the backscattering models used. These aspects are in the calibration performance monitoring philosophy. The major goals of the calibration monitoring activities are the achievement of a “flat” antenna pattern profile and the assurance of a stable absolute calibration level.

2.1 Gain Constant over transponder

One gain constant is computed per transponder per beam from the actual and simulated two-dimensional echo power, which is given as a function of the orbit time and range time. This parameter clearly indicates the difference between “real instrument” and the mathematic model. In order to acquire data over the transponder the Scatterometer must be set in an appropriate operational mode defined as “Calibration Mode”.

Since January 2001 with the operations in Zero Gyro Mode (ZGM) the satellite attitude is not stable as it was in the nominal Yaw Steering Mode (YSM). In particular there is a non-predictable variation of the yaw error angle along the orbit. For that reason the gain constant data computed by the CALPROC processor, that assumes a stable orbit, are meaningless and a new calibration processor is under development. In the mean time, data from the Transponder are still acquired and archived for future re-processing. The reprocessed gain constants will be provided in this section when available.

For the gain constant computed during the nominal YSM please refer to the Scatterometer cyclic report - cycle 60 -.

2.2 Ocean Calibration

The Scatterometer sigma noughts were compared with the ECMWF model first guess winds. The result is shown in Figure 1 as the ratio of <sigma_0^0.625>/<CMOD4(First Guess)^0.625> converted in dB for the for beam (solid line), mid beam (dashed line) and aft beam (dotted line), as a function of incidence angle for descending and ascending tracks. The thin lines indicate the error bars on the estimated mean. First-guess winds are based on the in time closest (+3h, +6h, +9h, or +12h) T511 forecast field, and are bilinearly interpolated in space.

The average sigma0 bias levels (compared to simulated sigma0’s based on ECMWF model first-guess winds) stratified with respect to antenna beam, ascending or descending track and as function of incidence angle (i.e. across-node number) is displayed in Figure 1. Compared to cycle 89, bias levels were nearly unchanged. Largest differences were observed at the near range descending tracks where levels have become 0.1 dB less negative. The situation is slightly better than that for nominal data in 2000 (see same figure of the ECMWEF cyclic reports for cycle 48 to 59).

The dependency of the bias as function of incidence angle is small, and the tendency of being somewhat more negative at the far range has been suppressed. In fact, now levels are most negative in the near range. Internode differences are slightly smaller than for the nominal period. Bias

levels are in between 0.0 and -0.5 dB. The data volume of ascending and descending tracks are similar.

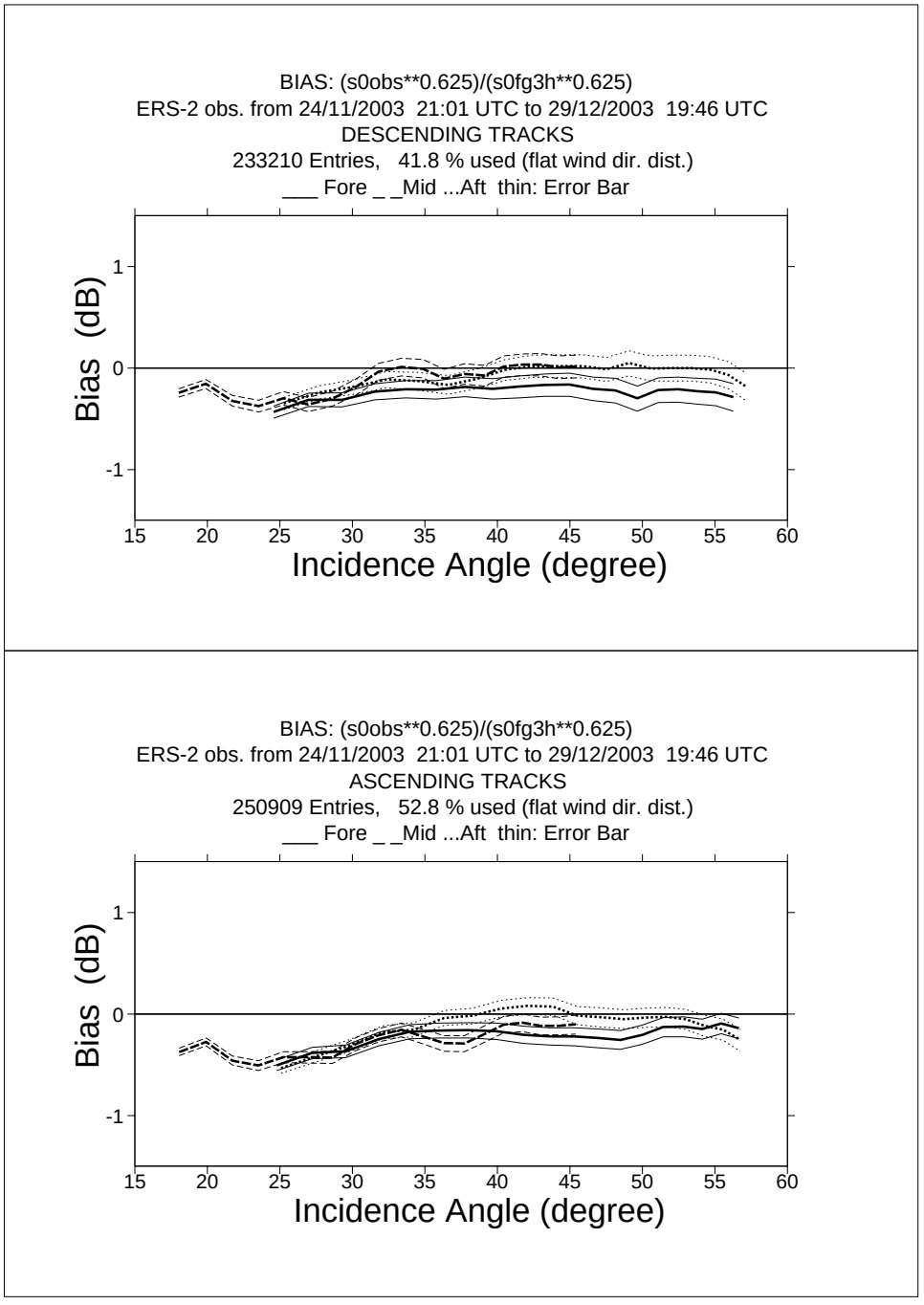

FIGURE 1. ERS-2 Scatterometer Ocean Calibration cycle 90. Ratio of <sigma_0^0.625>/<CMOD4(First Guess)^0.625> converted in dB for the fore beam (solid line), mid beam (dashed line) an aft beam (dotted line), as a function of incidence angle for descending and ascending tracks. The thin lines indicate the error bars on the estimated mean. First-guess winds are based on the in time closest (+3h, +6h, +9h, or +12h) T511 forecast field, and are bilinearly interpolated in space.

2.3 Gamma-nought over Brazilian rain forest

Although the transponders give accurate measurements of the antenna attenuation at particular points of the antenna pattern, they are not adequate for fine tuning across all incidence angles, as there are simply not enough samples. The tropical rain forest in South America has been used as a reference distributed target. The target at the working frequency (C-band) of ERS-2 Scatterometer acts as a very rough surface, and the transmitted signal is equally scattered in all directions (the target is assumed to follow the isotropic approximation). Consequently, for the angle of incidence used by ERS-2 Scatterometer, the normalised backscattering coefficient (sigma nought) will depend solely on the surface effectively seen by the instrument:

$$S^0 = S \bullet \cos\theta$$

With this hypothesis it is possible to define the following formula:

$$\gamma^0 = \frac{\sigma^0}{\cos\theta}$$

Using this relation, the gamma nought backscattering coefficient over the rain forest is independent of the incident angle, allowing the measurements from each of the three beams to be compared.

The test area used by the PCS is located between 2.5 degrees North and 5.0 degrees South in latitude and 60.5 degrees West and 70.0 degrees West in longitude. That area is actually not covered by the Regional mission scenario (since cycle 86 onwards) and therefore the calibration monitoring activity over the Brazilian rain forest is suspended because no data are available.

The chance to continue the monitoring activity with a new receiving station covering the Brazilian rain forest is under investigation. The following paragraphs will report on the results when data will be available.

2.3.1 Antenna pattern: Gamma-nought as a function of elevation angle

Due to the regional mission scenario data over the Brazilian rain forest are not available and the, the antenna patterns in function of the elevation angle have not been computed.

2.3.2 Antenna pattern: Gamma-nought as a function of incidence angle

Due to the regional mission scenario data over the Brazilian rain forest are not available and the, the antenna patterns in function of the incidence angle have not been computed

2.3.3 Gamma nought histograms and peak position evolution

As the gamma nought is independent from the incidence angle, the histogram of gamma noughts over the rain forest is characterised by a sharp peak. The time-series of the peak position gives some information on the stability of the calibration. This parameter is computed by fitting the histogram with a normal distribution added to a second order polynomial:

$$F\langle x\rangle = A_0 \cdot \exp\left(-\frac{z^2}{2}\right) + A_3 + A_4 \cdot x + A_5 \cdot x^2$$

where: $z = \dfrac{x - A_1}{A_2}$

The parameters are computed using a non linear least square method called “gradient expansion”. The position of the peak is given by the maximum of the function F(x). The histograms are computed weekly (from Monday to Sunday) for each antenna individually (“Fore”, “Mid”, and “Aft”) and for ascending and descending passes with a bin size of 0.02 dB.

Due to the regional mission scenario data over the Brazilian rain forest are not available and the, the histograms have not been computed.

For the time series since the beginning of the mission please refer to the Scatterometer cyclic report cycle 86.

2.3.4 Gamma nought image of the reference area

Due to the regional mission scenario data over the Brazilian rain forest are not available and the, the histograms have not been computed

2.3.5 Sigma nought evolution

Due to the regional mission scenario data over the Brazilian rain forest are not available and the, the sigma nought evolution have not been computed

For the time series since the beginning of the mission please refer to the Scatterometer cyclic report cycle 86.

2.3.6 Antenna temperature evolution over the Rain Forest

Due to the regional mission scenario data over the Brazilian rain forest are not available.

For the time series since the beginning of the mission please refer to the Scatterometer cyclic report cycle 86.

3.0 Instrument performance

The instrument status is checked by monitoring the following parameters:

- Centre of Gravity (CoG) and standard deviation of the received signal spectrum. This parameter is useful for the monitoring of the orbit stability, the performances of the doppler compensation filter, the behaviour of the yaw steering mode and the performances of the devices in charge for the satellite attitude (e.g. gyroscopes, Earth sensor, Sun sensor).
- Noise power I and Q channel.
- Internal calibration pulse power.

the latter is an important parameter to monitor the transmitter and receiver chain, the evolution of pulse generator, the High Power Amplifier (HPA), the Travelling Wave Tube (TWT) and the receiver.

These parameters are extracted daily from the UWI products and averaged. The evolution of each parameter is characterised by a least square line fit. The coefficients of the line fit are printed in each plot.

3.1 Centre of gravity and standard deviation of received power spectrum

The Figure 2 shows the evolution of the two parameters for each beam for the long term monitor and Figure 3 shows the same for the cycle 90.

The tendency from the beginning of the mission to the operation with the new Mono Gyro (MGM) Attitude On-board Control System (AOCS) configuration (7th February 2000) is a clear and regular small increase of the Centre of gravity (CoG) of received spectrum for the three antennae. An increase of roughly 200 Hz was observed at the end of the MGM qualification period. After the AOCS commissioning phase this parameter further evolved.

The nominal 3-gyroes AOCS configuration (plus one Digital Earth Sensor - DES, and one Digital Sun Sensor - DSS and backups) was no more considered safe because 3 of the six gyros on-board were out of order or very noisy. The MGM configuration was designed to pilot the ERS-2 using only one gyro plus the DES and the DSS modules. Scope of ZGM configuration was to extend the satellite lifetime by using the available gyros one at the time.

With MGM configuration, the gyro 5 was used until 7th October 2000 when it failed. From 10th October 2000 to 24th October 2000 the gyro 6 was used. This explains the decrease of roughly 100Hz in the CoG of the received spectrum. From 25th October 2000 to 17th January 2001 the gyro 1 was used to pilot the ERS-2 satellite.

On 17th January 2001 the AOCS was upgraded. The new configuration allows to pilot the satellite without gyroscopes. Unfortunately a failure of the Digital Earth Sensor (DES A-side) caused ERS-2 to enter in Safe-Mode on the same day. On 25th January 2001 gyro #1 also failed. During the period of safe mode the spacecraft had drifted out of the nominal deadband by some 30 Km. The nominal orbit was reached on 6th February 2001.

In order to preserve the remaining gyroscope for further manoeuvres, ERS-2 will now being operated in Extra Backup Mode (EBM). The EBM is a coarse attitude control mode. An upgrade of

EBM has been performed on 30th March 2001. The aim of the upgrade was to introduce the Yaw steering law inside the piloting function. The new configuration has been renamed as EBM-YSM.

Since 7th June 2001 a new AOCS configuration is active on board. The purpose of the Zero Gyro Mode (ZGM) is to improve the yaw performances without use of gyroscope.

Until 17th January 2001 the evolution of the standard deviation of the CoG of the received spectrum was stable apart from the change occurred on 26th, October 1998. On October 26th, 1998 the standard deviation of the CoG had, on average, a decrease of roughly 100 Hz for the fore and aft antenna and of roughly 30Hz for the mid antenna. This change is linked with the increase of the transmitted power (see Section 3.3).

Others changes in the AOCS configuration are recognised in Figure 2. The two steps observed at the beginning of the plots of the CoG (see Figure 2) are due to a change in the pointing subsystem (DES reconfiguration) side B instead of side A after a depointing anomaly (see table 1 for the list of the all AOCS depointing anomaly occurred during the ERS-2 mission). The first change is from 24th, January 1996 to 14th, March 1996, the second one is from 14th February 1997 to 22nd April 1997. During these periods side B was switched on. It is important to note that during the first time a clear difference in the CoG of the received spectrum is present only for the Fore antenna (an increase of roughly 100 Hz) while during the second time the change has affected all the three antennae (roughly an increase of 200 Hz, 50 Hz and 50 Hz for the fore, mid and aft antenna respectively).

Table 1: ERS-2 Scatterometer AOCS depointing anomaly

From	To
24th January 1996 9:10 a.m.	26th January 1996 6:53 p.m
14th February 1997 1:25 a.m.	15th February 1997 3:44 p.m
3rd June 1998 2:43 p.m.	6th June 1998 12:47 a.m.
1st September 1999 8:50 a.m.	2nd September 1999 1:28 a.m.
7th October 2000 4:38 p.m.	10th October 2000 4:49 p.m.
24th October 2000 4:05 p.m.	25th October 2000 12:05 p.m.
17th January 2001	6th February 2001

The Figure 2 shows also when the satellite was operated in Fine Pointing Mode (FPM) in EBM, ZGM mode or the on-board doppler compensation was missing. These events are related with the large peaks in the CoG of the received spectrum plots (fore and aft antenna) and are listed in Table 2.

Table 2: ERS-2 Scatterometer anomalies in the CoG fore and aft antenna

Date	Reason
26th and 27th September 1996	missing on-board doppler coefficient (after cal. DC converter test period)
6th and 7th June 1998	no Yaw Steering Mode (after depointing anomaly)

Date	Reason
2nd and 3rd December 1998	missing on-board doppler coefficients (after AMI anomaly 228)
16th and 17th February 2000	Fine Pointing Mode (FPM) (due to AOCS mono-gyro qualification period)
14th April 2000	Fine Pointing Mode (FPM)
30th May 2000	Fine Pointing Mode (FPM)
5th July 2000	Fine Pointing Mode (FPM) after instrument switch-on
27th September 2000	Fine Pointing Mode (FPM) to up-load AOCS software patch
2nd November 2000	Fine Pointing Mode (FPM)
5th and 6th December 2000	Fine Pointing Mode (FPM) due to orbital manoeuvre
6th February - 30th March 2001	Extra Backup Mode (EBM) coarse attitude control
30th March 2001- 7th June 2001	EBM-YSM gyro-less yaw steering mode
7th June 2001 - onwards	ZGM commissioning phase

The peaks (before February 2001) shown in the plot of mid beam standard deviation of the CoG of the received spectrum are linked to the satellite manoeuvres and AOCS depointing anomaly.

Since February 2003 (with the beta version of ESACA processor) the evolution of the Doppler compensation was stable. This because ESACA takes into account the real acquisition geometry and therefore is able to compensate for the received signal. The CoG is very close to zero and the standard deviation was reduced a lot: it was around 1800 Hz for Fore and Aft beam and around 2800 Hz for the mid beam.

During the cycle 90 the Doppler compensation evolution was stable (see Figure 3) apart from the small peak on day 26 November due to a set of orbit manoeuvres.

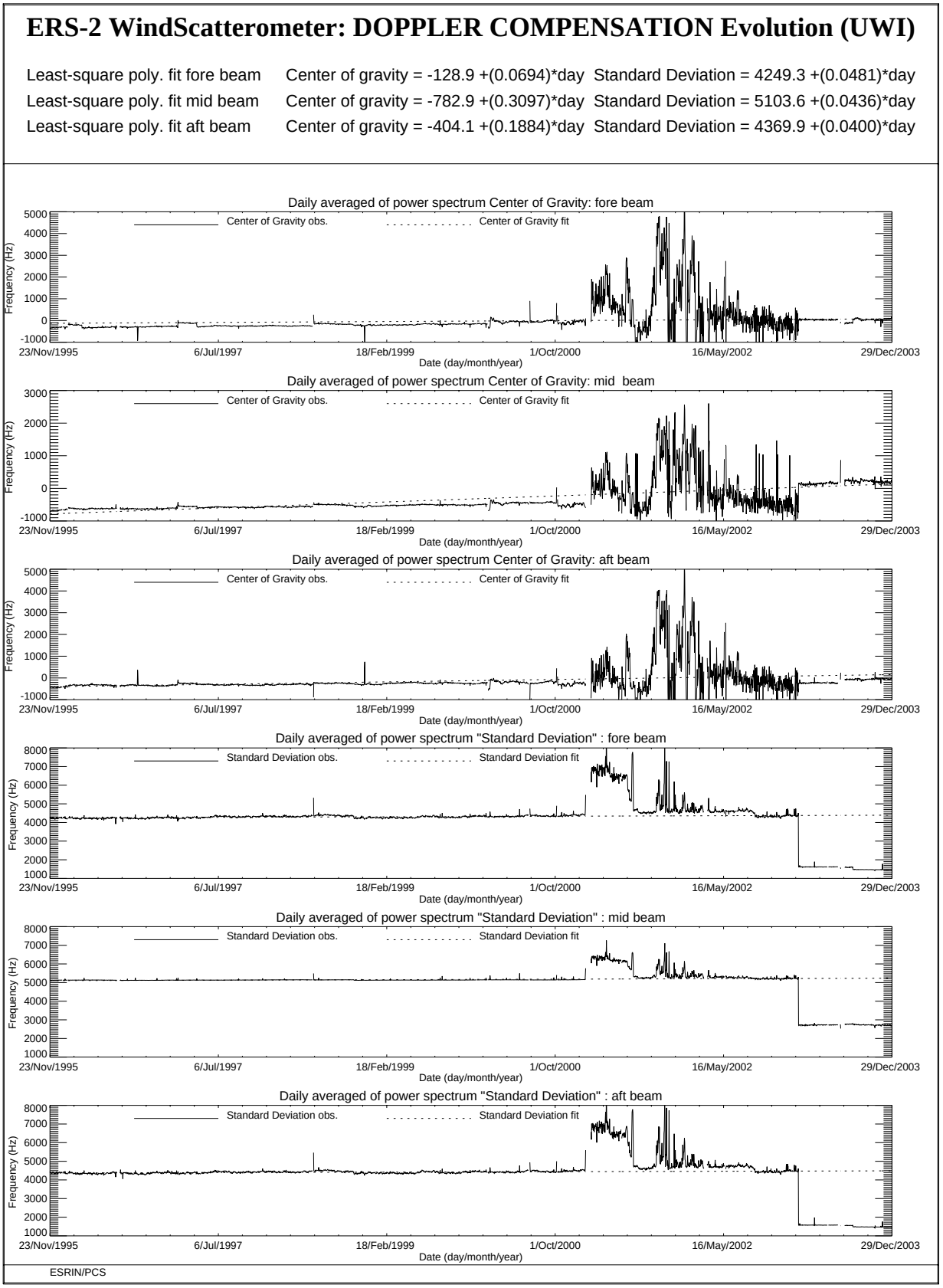

FIGURE 2. ERS-2 Scatterometer: Centre of Gravity and standard deviation of received power spectrum since the beginning of the mission.

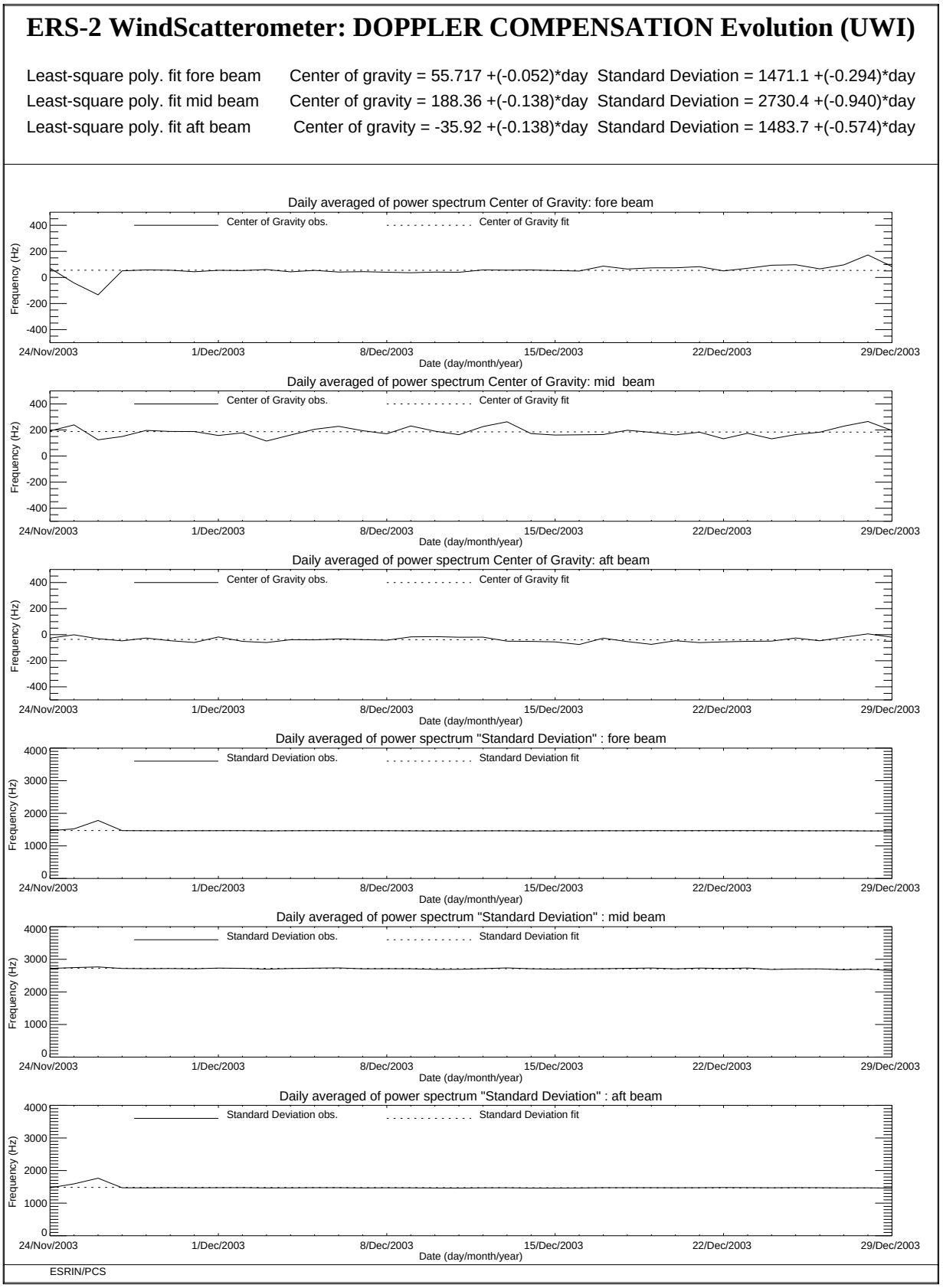

FIGURE 3. ERS-2 Scatterometer: Centre of Gravity and standard deviation of received power spectrum during the cycle 90.

3.2 Noise power level I and Q channel

The results of the monitoring are shown in Figure 4 (long-term) and Figure 5 (cycle 90). The first set of three plots presents the noise power evolution for the I channel while the second set shows the Q channel. The noise level is less than 1 ADC Unit for the fore and aft signals and is negligible for the mid one. From the plots one can see that the noise level is more stable in the I channel than in the Q one. The PCS suspects that an explanation should be found in the different position of the receivers, in particular it seems that the Q one is closer to the ATSR-GOME electronics. A confirmation of this hypothesis has been asked to ESTEC.

From 5th December 1997 until November 1998 some high peaks appear in the plots. These high values for the daily mean are due to the presence for these special days of a single UWI product with an unrealistic value in the noise power field of its Specific Product Header. The analysis of the raw data used to generate these products lead in all cases to the presence of one source packet with a corrupted value in the noise field stored into the source packet Secondary Header. The reason why noise field corruption is beginning from 5th December 1997 and last until November 1998 is at present unknown. It is interesting to note that at the beginning of December 1997, we started to get as well the corruption of the Satellite Binary Times (SBTs) stored in the EWIC product. The impact in the fast delivery products was the production of blank products starting from the corrupted EWIC until the end of the scheduled stop time. A change in the ground station processing in March 1998 overcame this problem.

Since 9th August 1998 until March 2000 some periods with a clear instability in the noise power have been recognised. Table 5 gives the detailed list.

Table 3: ERS-2 Scatterometer instability in the noise power

From	To
9th August 1998	26th October 1998
29th November 1998	6th December 1998
23rd December 1998	24th December 1998
7th June 1999	10th June 1999
17th August 1999	22nd August 1999
8th September 1999	9th September 1999
3rd October 1999	8th October 1999
16th October 1999	18th October 1999
26th October 1999	28th October 1999
25th December 1999	2nd January 2000
10th February 2000	11th February 2000
19th March 2000	26th March 2000

To better understand the instability of the noise power the PCS has carried out investigations in the scatterometer raw data (EWIC) to compute the noise power with more resolution. The result is that for the orbits affected by the instability the noise power had a decrease of roughly 0.7 dB for

the fore and aft signals and a decrease of roughly 0.6 dB in the mid beam case (see the report for the cycle 42).

The decrease of the noise power during the orbits affected by the instability is comparable with the decrease of the internal calibration level that occurred during the same orbits. The reason of this instability (linked to the AMI anomalies) is still under investigation. A plot that shows the correlation among the noise power, the internal calibration level and the AMI anomaly is reported in section 3.3.

The noise power decrease noted on 6th June 2001 is related with continuous wave operation around the orbit. The reduction of the noise is an artifact due to on-board data processing. In fact all noise samples taken during 32 FMA sequence are squared and averaged over 896 samples. In wind-wave mode 2 FMA sequences are missing (to acquire SAR imagette) but the average is still computed over 896 samples (see ER-SS-MSS-AM-0700 sheet 167).

On 28th February 2003 the Scatterometer receiver gain has been increased by 3 dB to increase the usage of the on-board ADC converter. This explains the increase of the noise for the Fore and Aft beam channel. For the mid beam channel the noise still remains not measurable.

The evolution of the noise power during the cycle 90 was stable (see Figure 5). The daily average for the Fore and Aft beam noise is around 1.7 ADC and for the Mid beam the noise is not measurable.

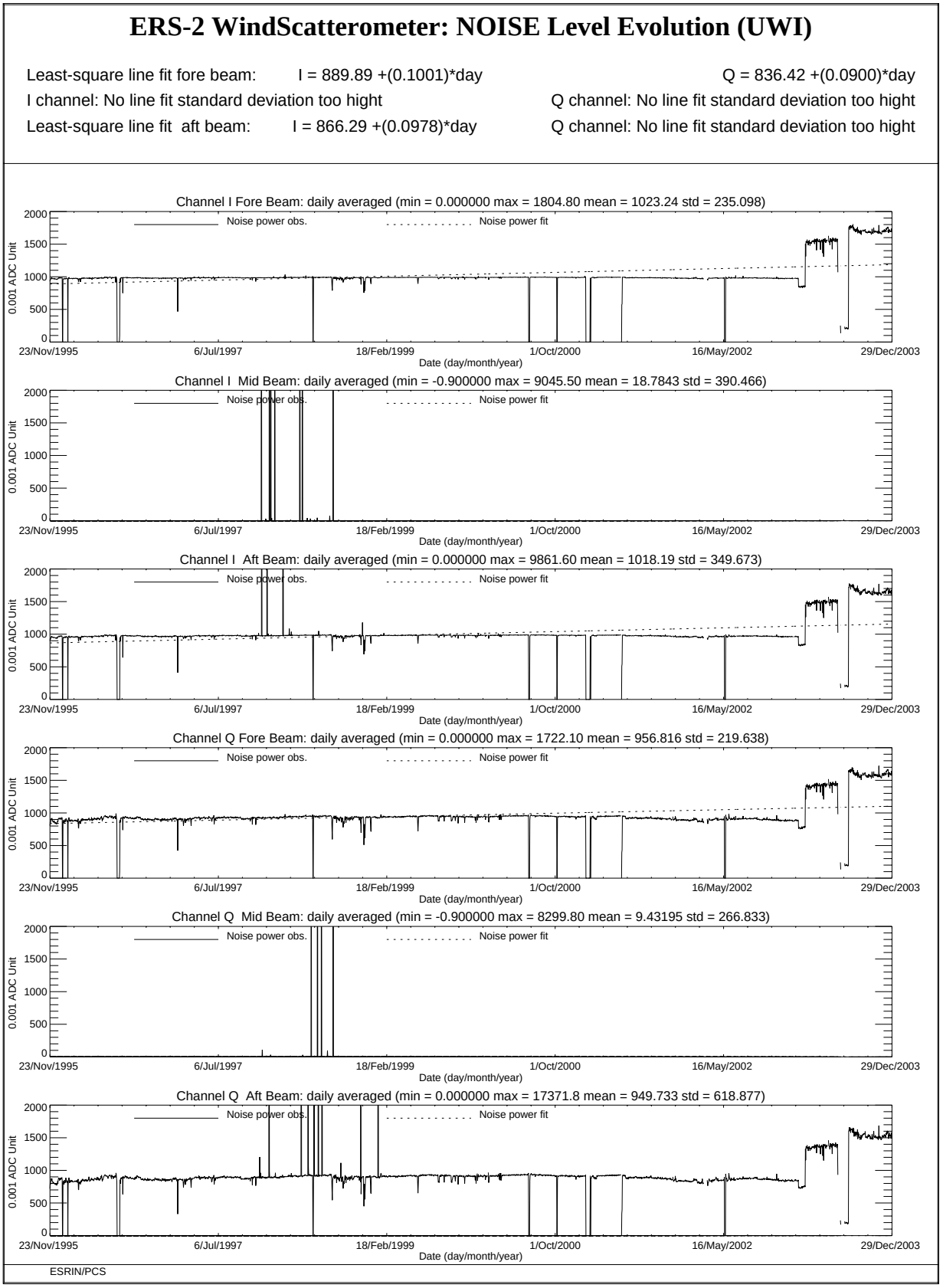

FIGURE 4. ERS-2 Scatterometer: noise power I and Q channel since the beginning of the mission.

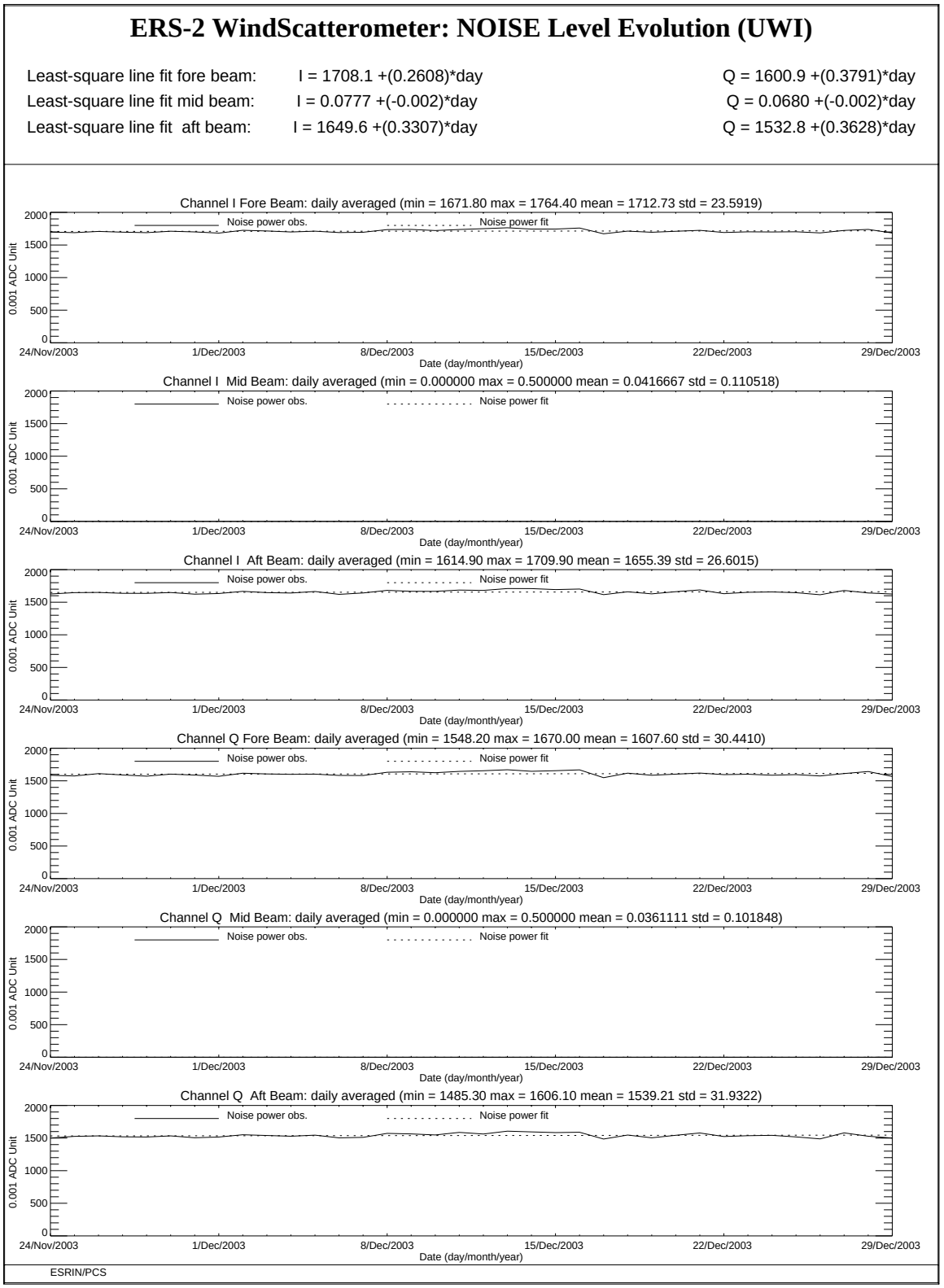

FIGURE 5. ERS-2 Scatterometer: noise power I and Q channel for cycle 90.

3.3 Power level of internal calibration pulse

For the internal calibration level, the results are shown in Figure 6 (long-term) and Figure 7 (cycle 90).

The high value of the variance in the fore beam until August, 12th 1996 is due to the ground processing. In fact all the blank source packets ingested by the processor were recognized as Fore beam source packets with a default value for the internal calibration level. The default value was applicable for ERS-1 and therefore was not appropriate for ERS-2 data processing. On August 12th, 1996 a change in the ground processing LUT overcame the problem.

Since the beginning of the mission a power decrease is detected. The power decrease is regular and affects the AMI when it is working in wind-only mode, wind/wave mode and image mode indifferently. The average power decrease is around 0.08 dB per cycle (0.0022 dB/day) and is more clear after August, 6th 1996 when the calibration subsystem has been changed.

The reason of the power decrease is because the TWT is not working in saturation, so that a variation in the input signal is visible in the output. The variability of the input signal can be two-fold: the evolution of the pulse generator or the tendency of the switches between the pulse generator and the TWT to reset themselves into a nominal position. These switches were set into an intermediate position in order to put into operation the scatterometer instrument (on 16th November 1995).

To compensate for this decrease, on 26th October 1998 (cycle 37) 2.0 dB were added to the Scatterometer transmitted power and on 4th September 2002 (cycle 77) were added 3.0 dB. On 28th February 2003 (cycle 82) the Scatterometer receiver gain was increased by 3 dB to improve the usage of the on-board ADC converter. These events are clearly displayed by the large steps shows in Figure 6.

Since 9th August 1998 until March 2000 the internal calibration level shows an instability after an AMI or platform anomaly (see reports from cycle 35 to cycle 52). This instability is very well correlated with the fluctuations observed in the noise power as outlined in section 3.2. T

On 13th July 2000 an high peak (+3.5 dB) was detected in the transmitted power. This event has been investigated deeply by PCS and ESOC. The results of the analysis are reported in the technical note “ERS-2 Scatterometer: high peak in the calibration level” available in the PCS. The high transmitted power was detected after an arcing event which occurred inside the HPA. After that event the calibration level had an average increase of roughly 0.14 dB.

During the cycle 90 the mean power decrease has been 0.13 dB per cycle.That value is within the trend detected since the beginning of the mission.

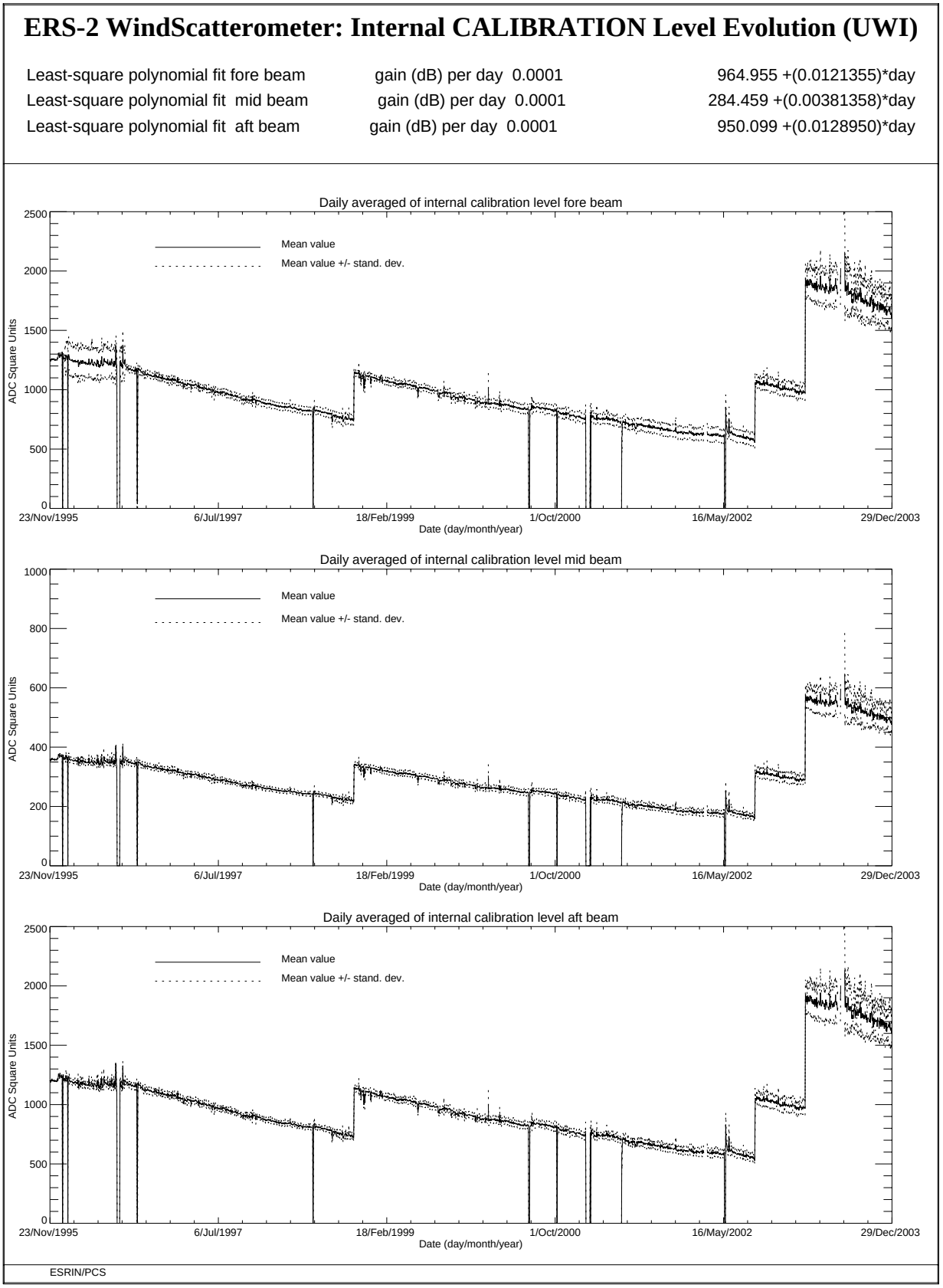

FIGURE 6. ERS-2 Scatterometer: power of internal calibration pulse since the beginning of the mission.

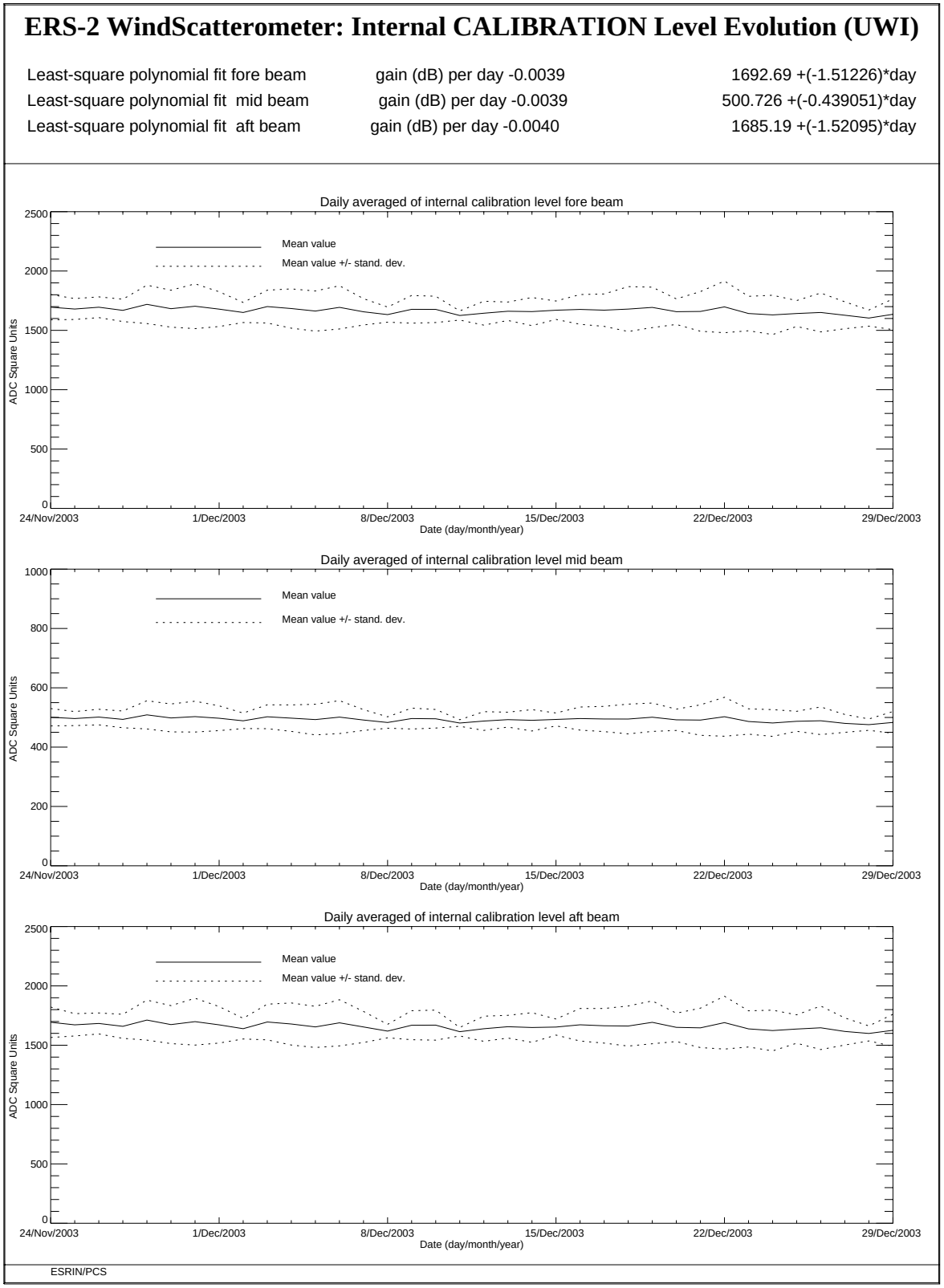

FIGURE 7. ERS-2 Scatterometer: power of internal calibration level cycle 90.

4.0 Products performance

The PCS carries out a quality control of the winds generated from the WSCATT data. External contributions to this quality control (from ECMWF) are also reported in this chapter.

4.1 Products availability

One of the most important point in the monitoring of the products performance is their availability. The Scatterometer is a part of ERS payload and it is combined with a Synthetic Aperture Radar (SAR) into a single Active Microwave Instrument (AMI). The SAR users requirements and the constraints imposed by the on-board hardware (e.g. amount of data that can be recorded in the on-board tape) set rules in the mission operation plan.

The principal rules that affected the Scatterometer instruments are:

- over the Ocean the AMI is in wind/wave mode (scatterometer with small SAR imagettes acquired every 30 sec.) and the ATSR-2 is in low rate data mode.
- over the Land the AMI is in wind only mode (only scatterometer) and the ATSR-2 is in high rate mode. (Due to on board recorder capacity, ATSR-2 in high rate is not compatible with Sar wave imagette acquisitions.)

This strategy preserves the Ocean mission.

Moreover:

- the SAR images are planned as consequence of users' request.

These rules have an impact on the Scatterometer data availability.

Since July 16th 2003 the ERS-2 Low Rate mission is continued within only the visibility of ESA ground stations over Europe, North Atlantic, the Arctic and western North America. The reason was the failure of both on-board tape recorders.

In order to maximize the data coverage, since September 7th 2003 the ground station in Maspalomas, Gatineau and Prince Albert are acquiring and processing data for all the ERS-2 satellite passes within the station visibility (apart from passes for which other satellites have an higher priority). To further increase the wind coverage of the North Atlantic area, since December 8th, 2003 is operative a new ground Station in West Freugh (UK) and data from this new station are available to the user since mid January 2004. Due to its location, the West Freugh acquisitions have some overlap with those from three other ESA stations, Kiruna, Gatineau or Maspalomas. The station overlap depends on the relative orbit of the satellite. Consequentially, overlapping wind scatterometer LBR data may be included in two products. Since the two products are generated at different ground stations the overlap may not be completely precise, with a displacement up to 12 Km and slight differences in the wind data itself.

Figure 8 shows the AMI operational modes for cycle 90. Each segment of the orbit has different colour depending on the instrument mode: brown for wind only mode, blue for wind-wave mode and green for image mode. The red and yellow colours correspond to gap modes (no data acquired). Due to ZGM commissioning phase the AMI was operated in wind-wave mode through-

out the orbits. For cycle 90 the percentage of the ERS-2 AMI activity is shown in table 4. The numbers are in the nominal range.

Table 4: ERS-2 AMI activity (cycle90)

AMI modes	ascending passes	descending passes
Wind and Wind-Wave	**95.32%**	**81.46%**
Image	**2.70%**	**14.96%**
Gap and others	**1.98%**	**3.58%**

Table 5 reports the major data lost due to the test periods, AMI and satellite anomalies or ground segment anomalies occurred after 6thAugust, 1996 (before that day for many times data were not acquired due to the DC converter failure).

Table 5: ERS-2 Scatterometer mission major data lost after 6th, August 1996

Start date	Stop date	Reason
September 23rd, 1996	September 26th, 1996	ERS-2 switched off due to a test period
February 14th, 1997	February 15th, 1997	ERS-2 switched off due to a depointing anomaly
June 3^{rd,} 1998	June 6th, 1998	ERS-2 switched off due to a depointing anomaly
November 17th, 1998	November 18th, 1998	ERS-2 switched off to face out Leonide meteo storm
September 22nd 1999	September 23rd 1999	ERS-2 switched off due to Year 2000 certification test
November 17th, 1999	November 18th, 1999	ERS-2 switched off to face out Leonide meteo storm
December 31st,1999	January 2nd, 2000	ERS-2 switched off Y2K transition operation
February 7th,2000	February 9th, 2000	ERS-2 switched off due to new AOCS s/w up-link
June 30th, 2000	July 5th, 2000	ERS-2 Payload switched-off after RA anomaly
July 10th, 2000	July 11th, 2000	ERS-2 Payload reconfiguration
October 7th, 2000	October 10th, 2000	ERS-2 Payload switched-off after AOCS anomaly
January 17th, 2001	February 5th, 2001	ERS-2 Payload switched-off due to AOCS anomaly
May 22nd, 2001	May 24th, 2001	ERS-2 Payload switched-off due to platform anomaly
May 25th, 2001	May 25th, 2001	AMI switched-off due thermal analysis
November 17th, 2001	November 18th, 2001	ERS-2 switched off to face out Leonide meteo storm
November 27th, 2001	November 28th, 2001	ERS-2 payload off due to 1Gyro Coarse Mode commissioning
March 8th, 2002	March 20th, 2002	ERS-2 payload unavailability after RA anomaly
May 19th,2002	May 24th, 2002	AMI switched-off due to arc events
May 24th, 2002	May 28th, 2002	AMI partially switched-off due to arc events
May 31st, 2002	June 3rd, 2002	Gatineau orbits partially acquired due to antenna problem
June 4th, 2002	June 5th, 2002	AMI partially switched-off due to arc events
July 25th, 2002	July 25th, 2002	AMI switched off HPA voltage too low

Start date	Stop date	Reason
September 11th, 2002	September 11th, 2002	AMI switched off macrocommand transfer error
November 17th, 2002	November 18th, 2002	ERS-2 switched off to face out Leonide meteo storm
December 9th, 2002	December 10th, 2002	IDHT anomaly no data recorded on board
December 20th, 2002	December 20th, 2002	IDHT anomaly no data recorded on board
January 14th, 2003	January 14th, 2003	IDHT anomaly no data recorded on board
June 22nd, 2003	July 16th, 2003	IDHT recorders test no data acquired
July 16th, 2003	onwards	Data available only within the visibility of ESA ground station

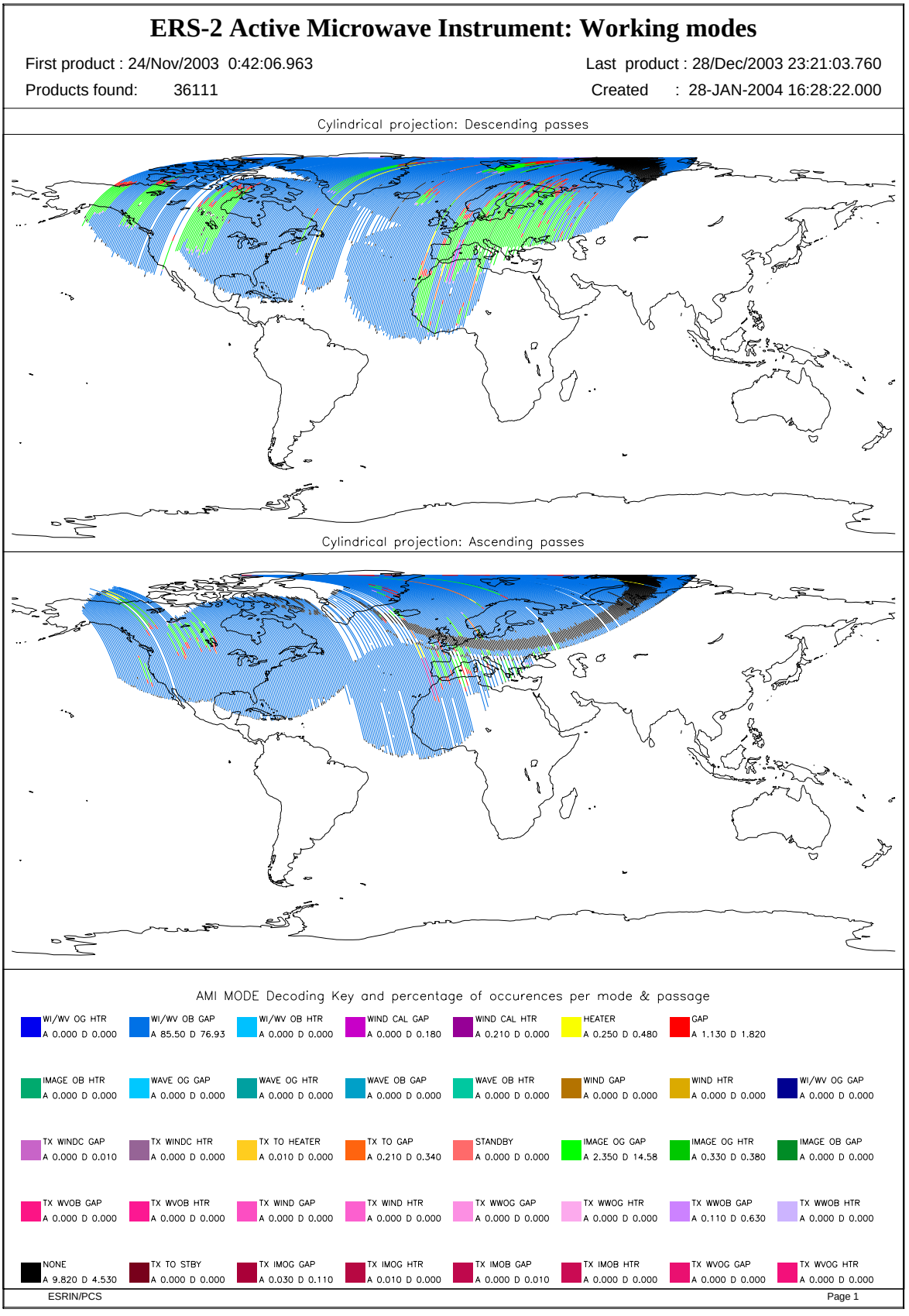

FIGURE 8. ERS-2 AMI activity during cycle 90.

4.2 PCS Geophysical Monitoring

The routine analysis is summarized in the plots of figure 9; from top to bottom:

- the monitoring of the valid sigma-nought triplets per day.
- the evolution of the wind direction quality. The ERS wind direction (for all nodes and only for those nodes where the ambiguity removal has worked properly) is compared with the ECMWF forecast. The plot shows the percentage of nodes for which the difference falls in the range -90.0, +90.0 degrees.
- the monitoring of the percentage of nodes whose ambiguity removal works successfully.
- the comparison of the wind speed deviation: (bias and standard deviation) with the ECMWF forecast.

The results since August 6th, 1996 until the beginning of the operation with the Zero Gyro Mode (ZGM) in January 2001 can be summarized as:

- High quality wind products has been distributed since Mid March 1996 (end of calibration and validation phase)
- The number of valid sigma-nought distributed per day was almost stable with a small increase after June 29th, 1999 due to the dissemination in fast delivery of the data acquired in the Prince Albert station.
- The wind direction is very accurate for roughly 93% of the nodes, the ambiguity removal processing successfully worked for more than 90.0% of the nodes.
- The UWI wind speed shows an absolute bias of roughly 0.5 m/s and a standard deviation that ranges from 2.5 m/s to 3.5 m/s with respect to the ECMWF forecast.
- The wind speed bias and its standard deviation have a seasonal pattern due to the different winds distribution between the winter and summer season.
- Two important changes affect the speed bias plot.
- the first is on June 3rd, 1996 due to the switch from ERS-1 to ERS-2 data assimilation in the meteorological model.
- the second which occurred at the beginning of September 1997, is due to the new monitoring and assimilation scheme in ECMWF algorithms (4D-Var).
- Since 19th April 1999 two set of meteo-table (meteorological forecast centred at 00:00 and 12:00 of each day) are used in the ground processing. This allowed the processing of wind data with 18 and 24 hours meteorological forecast instead of the 18, 24, 30 36 hours forecast. The comparison between data processed with the 18-24 hours forecast instead of 30-36 hours forecast shown an increase in the number of ambiguity removed nodes with a neutral impact in the daily statistics.
- The mono-gyro AOCS configuration (see report for cycle 50) that was operative from 7th February 2000 to 17th January 2001 did not affect the wind data performance.

During the Zero Gyro Mode (ZGM) phase the dissemination of the fast delivery scatterometer data to the users has been interrupted on 17th January 2001 due to degraded quality in sigma noughts and winds. The satellite attitude in ZGM is slightly degraded and the “old” ground processor was not able to produce calibrated data anymore. For that reason a re-design of the entire

ground processing has been carried out and since August 21st 2003 the new processor named ERS Scatterometer Attitude Corrected Algorithm (ESACA) is operative in all the ESA ground station and data was redistributed to the user.

Altought for a long period data was not distributed, the PCS has monitored the data quality (as shown in Figure 9) and the results during that period can be summarized as:

At the beginning of the ZGM (January 2001 - end July 2001) the number of valid nodes has a clear drop from 190000 per day to 9000 per day. This because the satellite attitude was strong degraded and the received signal had a very high Kp figure (in particular for the far range nodes). For the valid nodes, due to no calibrated sigma nought, the quality of the wind was very poor, the distance from the cone was high and the wind speed bias was above 1.5 m/s.

At the end of July 2001 the ZGM has been tuned and the satellite attitude had an improvement. This explain the increase of the number of valid nodes (returned around the nominal level) and the improvements in the wind speed bias (around 0.5 m/s).

On 4th February 2003, a beta version of the new ESACA processor has been put in operation in Kiruna for validation and the monitoring of the data quality has been done only for the new ESACA data. The number of valid nodes slight decreased because Kiruna station process only 9 of 14 orbits per day. The wind speed direction deviation had a clear improvement because ESACA implements a new ambiguity removal algorithm (MSC) and the ambiguity removal rate is now stable at 100% (the MSC is able to remove ambiguity for all the nodes). The wind speed bias had a clear drop from 0.5 to -0.5 m/s. That value is closer to the nominal one (around -0.2 m/s). As reported in the previous cyclic reports the beta version of ESACA had some calibration problem for the near range nodes and this explains why the data quality does not match exactly the one obtained in the nominal YSM. That problem has been overcame with the final release of the ESACA processor put into operation on August 21st 2003.

On June 22nd the failure of the on-board tape recorder discontinued the ERS global mission (see section 4.1) and this explains the low number of valid nodes available after that day.

Currently the performances of ESACA winds are affected by land contamination. Around costal zones many Sea nodes have a strong contribution of Land backscattering and the retrieved wind is not correct. An optimization of the Land/Sea flag in the ground processing is under investigation.

The statistics computed by PCS on the fast delivered winds are affected by Land and Ice contamination and for that reason the values of the wind speed bias and standard deviation are higher than nominal. With the global mission scenario that effect was present but it was negligible due to the large amount of data used to compute the statistics. A more refined Land mask used in the ground segment and the introduction of an Ice detection algorithm will improve the quality of the wind monitoring statistics.

Performances of ESACA winds without land contamination are given in section 4.3. In that case ECMWF removes from its analysis the wind nodes affected by Land and Ice backscattering. As shown in section 4.3 the performances of ESACA winds are similar to the ones obtained in the nominal YSM phase.

.

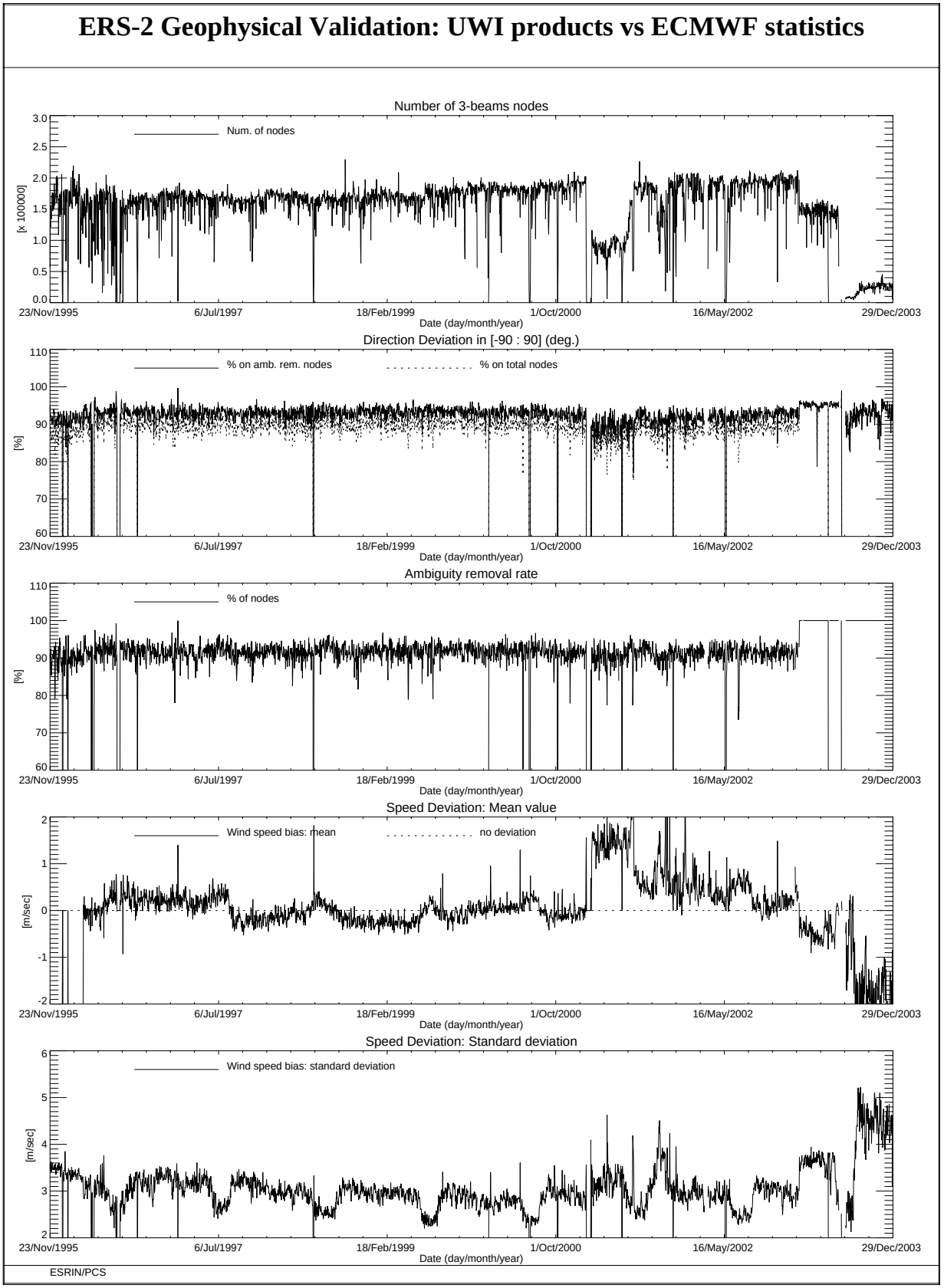

FIGURE 9. ERS-2 Scatterometer: wind products performance since the beginning of the mission.

4.3 ECMWF Geophysical Monitoring

On 21 August 2003, the world-wide dissemination of ERS-2 data was restarted. Due to a failure of both on-board LBR tape recorders two months earlier, only data is being received for data within the visibility range of a ground station. In practice this limits coverage to the North-Atlantic, part of the Mediterranean, the Gulf of Mexico, and to a small part of the Pacific north-west from the US and Canada (see Figure 10). Since 8 December 2003, a new ground station became operational in West Freugh (Scotland, UK), filling the gap in the data coverage in the North-Atlantic. However, during cycle 90, data from this station was not received at ECMWF (note from ESRIN: data was not disseminated to the user due to technical problem in ESRIN but are available), so the gap remained (see Figure 10).

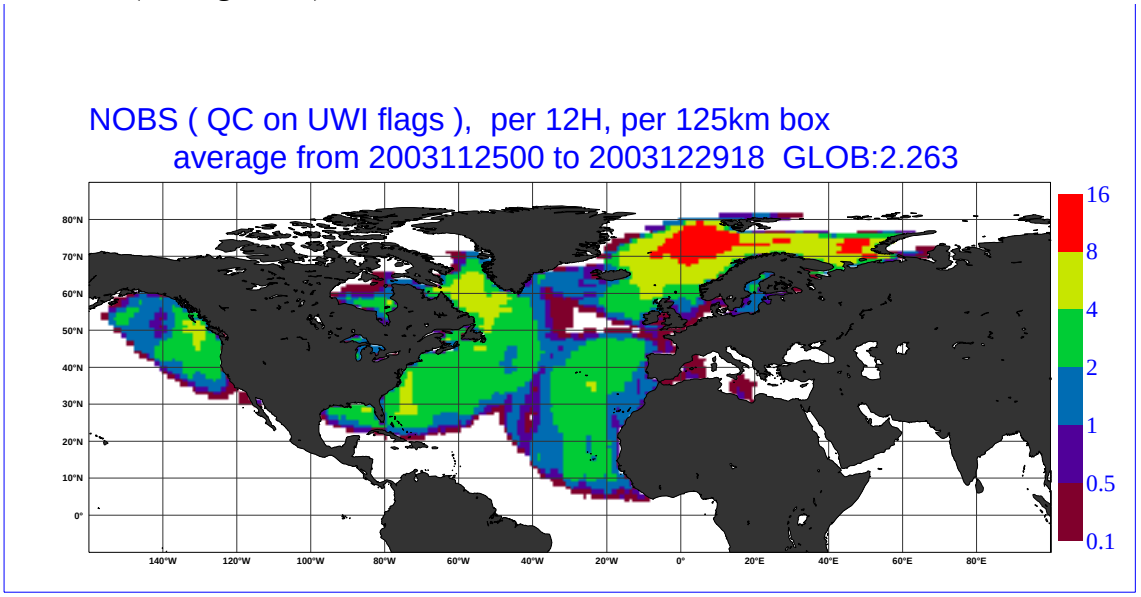

FIGURE 10. Average number of observations per 12H and per 125km grid box for UWI winds that passed the UWI flags QC and a check on the collocated ECMWF land and sea-ice mask.

The quality of the UWI product was monitored at ECMWF for cycle 90. Results were compared to those obtained from the previous cycle, as well for data received during the nominal period in 2000 (up to cycle 59). The ERS-2 scatterometer data was not used in the 4D-Var data assimilation system at ECMWF. However, it is being processed passively in the operational suite and assimilated actively (on the basis of CMOD5) in the experimental suite that is scheduled to become operational within a few months. During cycle 90, data was received between 21:01 UTC 24 November and 19:46 UTC 29 December 2003. No data was received for the 6-hourly batch centered around 06 UTC 03 December 2003 (note added by ESRIN: fast delivery dissemination problem for orbits from 45062 to 45065. Raw data was archived and available for re-processing). Due to an internal software problem at ECMWF, data was not available for the period between 18 UTC 08 December and 06 UTC 12 December 2003.

With some exceptions, the asymmetry between fore and aft incidence angles was within bounds. On 26 November 2003 deviations were larger than average (up to 7 degrees for node 10) and the combined Kp and yaw-error flag was set for most data received during that day. This anomaly in yaw steering control was not induced by solar activity (note added by ESRIN: it was due to orbital manoeuvres performed on that day). In fact, no periods of significantly enhanced solar activity were observed during cycle 90.

Compared to cycle 89, the agreement with ECMWF first-guess (FGAT) fields was somewhat worse. Although relative bias levels have been slightly reduced (from -0.55 m/s to -0.51 m/s), scatter has increased (from 1.59 m/s to 1.65 m/s). One should note, however, that due to the lack of global coverage, this trend is likely to be a result of seasonal variations. The quality of the UWI wind direction has improved. After the negative trend observed for cycle 89, performance is back on the level of cycle 88. The quality of de-aliased CMOD4 winds (that did not show a degradation for cycle 89) remained the same. Compared to nominal data in 2000, both backscatter and wind speed bias levels are somewhat more optimal. Internode and inter-beam dependent trends were found to be similar to the old situation. Standard deviations of wind speed are less optimal to those for 2000. A fair comparison, however, cannot be made due to large differences in data coverage.

The ECMWF assimilation system was not changed during cycle 90.

4.3.1 Distance to cone history

The distance to the cone history is shown in Figure 11.

Compared to cycle 89, average levels have increased from 1.18 to 1.23 and are now about 13% higher than for nominal data (see top panel Figure 9). This trend may be linked to the seasonal trend of the underlying wind climate. Time series are (due to lack of statistics) noisy, especially for the first nodes. This makes it difficult to identify peaks that might indicate a low data quality.

Most spikes appear at very low data volumes.

4.3.2 UWI minus First-Guess history

In Figure 12, the UWI minus ECMWF first-guess wind-speed history is plotted. Curves are based on data that passed all QC, including the test on the Kp -yaw flag, however subject to the land and sea-ice check at ECMWF (see cyclic report 88 for details). The history plot shows many peaks, most of them being a result of low data volume. Other ones indicate a real discrepancy between UWI and ECMWF winds. An example is shown for 01 UTC 22 December 2003 near the Labrador sea. It presents a situation in which UWI and ECMWF are nearly orthogonal. There are clearly some problems with the dealising algorithm, although due to the large difference in wind direction. Average bias levels and standard deviations of UWI winds relative to FGAT winds are displayed in Table 6.

Table 6: Biases and standard deviation of ERS-2 versus ECMWF FGAT winds in m/s for speed and degrees for direction

	Cycle 89 UWI	Cycle 89 CMOD-4	Cycle 90 UWI	Cycle 90 CMOD-4
speed stdev	1.59	1.58	1.65	1.63
node 1-2	1.59	1.55	1.63	1.58
node 3-4	1.51	1.50	1.56	1.54
node 5-7	1.50	1.50	1.56	1.56
node 8-10	1.54	1.54	1.60	1.59

Table 6: Biases and standard deviation of ERS-2 versus ECMWF FGAT winds in m/s for speed and degrees for direction

	Cycle 89 UWI	Cycle 89 CMOD-4	Cycle 90 UWI	Cycle 90 CMOD-4
node 11-14	1.58	1.58	1.61	1.61
node 15-19	1.62	1.61	1.68	1.68
speed bias	-0.55	-0.53	-0.51	-0.49
node 1-2	-1.17	-1.14	-1.21	-1.16
node 3-4	-0.89	-0.82	-0.89	-0.81
node 5-7	-0.58	-0.54	-0.56	-0.52
node 8-10	-0.36	-0.34	-0.32	-0.31
node 11-14	-0.31	-0.31	-0.28	-0.28
node 15-19	-0.34	-0.35	-0.24	-0.23
direction stdev	36.2	19.9	29.3	19.8
direction bias	-2.3	-2.8	-3.3	-2.9

From this it is seen that the bias of both the UWI and CMOD4 product have been reduced by 0.04 m/s. However, internode differences have, again, become larger, being most negative in the near range. The average bias level is better than for nominal data in 2000 (UWI: -0.51 m/s now, was -0.79 m/s for cycle 59). Although bias levels have become more optimal, the standard deviation of UWI winds compared to cycle 89 has worsened (1.65 m/s, was 1.59 m/s). This increase is similar for all nodes. Like for nominal data, lowest scatter is achieved around node 5. The observed trends in the UWI wind product may be a result of the in time changing wind climate for the now regional data. For cycle 90 the (UWI - model) direction standard deviations were ranging between 20 and 40 degrees (Figure 12). Sharp peaks are the result of low data volumes. For de-aliased CMOD4 winds values between 20 and 30 degrees are most common (Figure 15). With respect to cycle 89, the average standard deviation (see Table 6) of the UWI wind direction has improved (29.3 degrees, was 36.2 degrees) and is therefore back on the level of cycle 88. The lower performance during cycle 89 was mainly caused by the period between 4 and 20 November 2003 (see previous cyclic report). The quality of the de-aliased CMOD4 wind direction is stable (19.8 degrees, was 19.9 degrees). Bias levels in wind direction have become more negative for UWI winds (-3.3 degrees, was -2.3 degrees) but was stable for de-aliased CMOD4 winds (-2.9 degrees, was -2.8 degrees).

4.3.3 Scatter plots

Scatterplots of model 10 m first-guess winds versus ERS-2 winds are displayed in Figures 16 to 18. Values of standard deviations and biases are slightly different from those displayed in Table 6. Reason for this is that, for plotting purposes, the in 0.5 m/s resolution ERS-2 winds have been slightly perturbed (increases scatter with 0.02 m/s), and that zero wind-speed ERS-2 winds have been excluded (decreases scatter with about 0.05 m/s). The scatterplot of UWI wind speed versus FGAT (Figure 16) is very similar to that for (at ECMWF inverted) de-aliased CMOD4 winds (Figure 18). It confirms that the ESACA inversion scheme is working properly. The standard deviation for the CMOD4 winds is higher than for cycle 89 (1.66 m/s was 1.61 m/s), probably the re-

sult of the more extreme winds encountered in winter time. The UWI wind bias, has been reduced (-0.51 m/s, was -0.55 m/s). The average bias of the UWI wind direction was nearly unchanged (Figure 13, -3.2 degrees, was -3.0 degrees), as can be seen from Figure 17 Standard deviation in UWI wind direction has become lower (27.7 degrees, was 33.2 degrees).Winds derived on the basis of CMOD5 are displayed in Figure 19. The bias compared to FGAT winds remains small (0.06 m/s, was 0.01 m/s). The quality of these winds is higher than that of the CMOD4 winds.

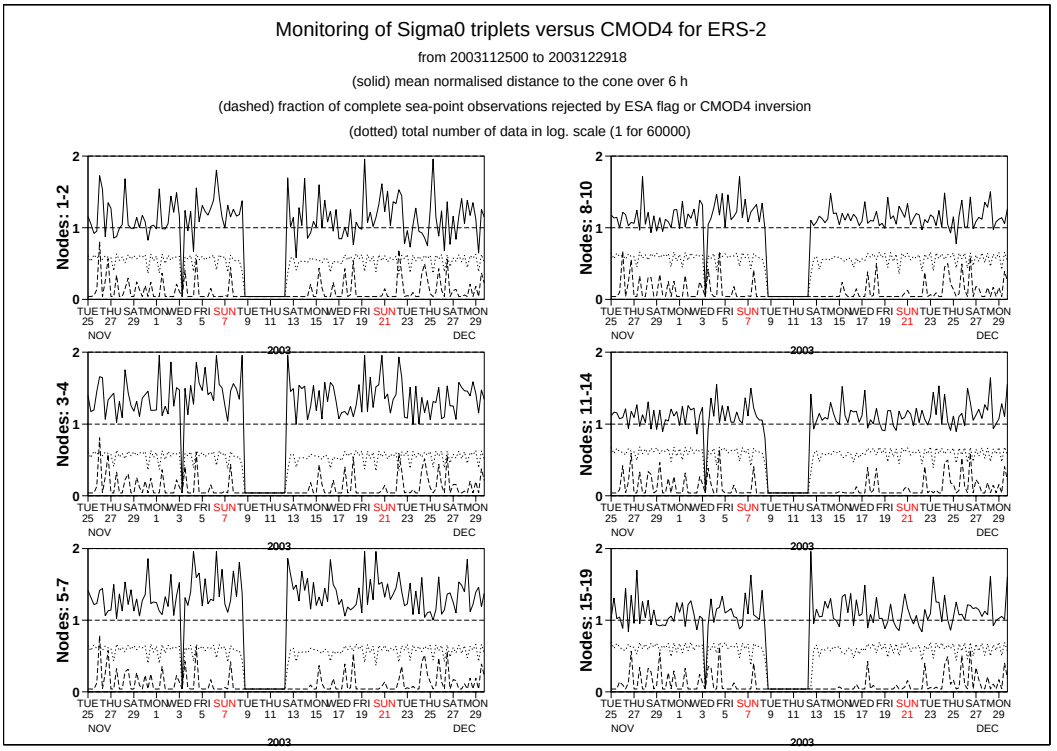

FIGURE 11. Mean normalised distance to the cone computed every 6 hours for nodes 1-2, 3-4, 5-7, 8-10, 11-14 and 15-19 (solid curve close to 1 when no instrumental problems are present). The dotted curve shows the number of incoming triplets in logarithmic scale (1 corresponds to 60,000 triplets) and the dashed one indicates the fraction of complete sea-located triplets rejected by the ESA flag, or by the wind inversion algorithm (0: all data kept, 1: no data kept). Cycle 90

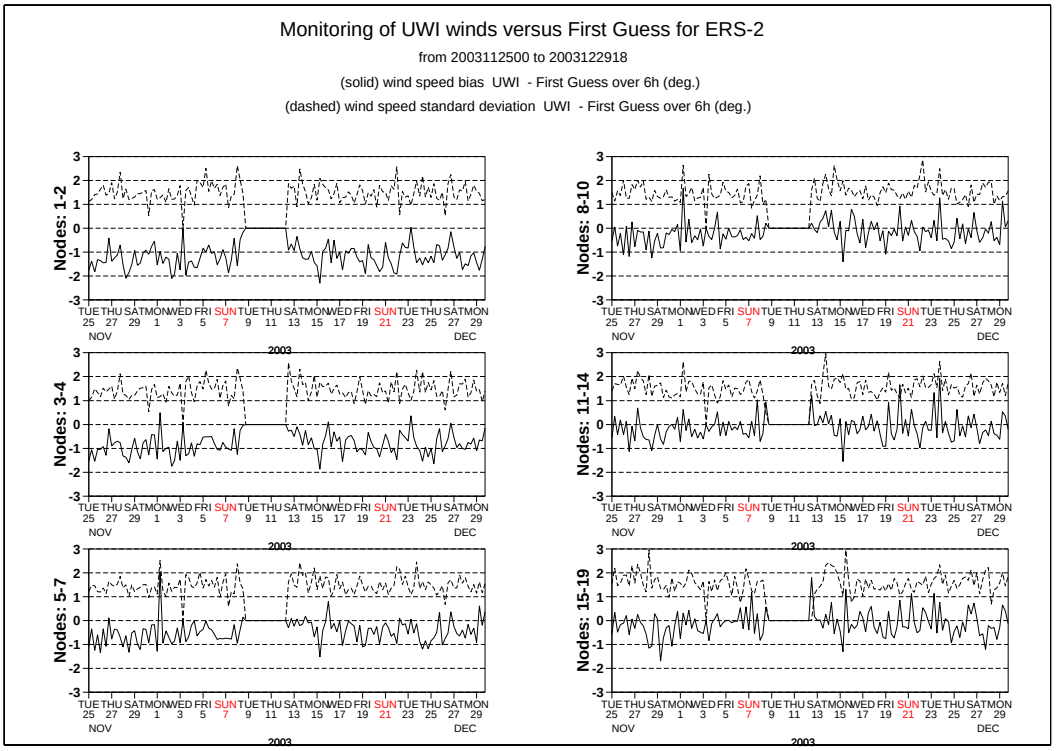

FIGURE 12. Mean (solid line) and standard deviation (dashed line) of the wind speed difference UWI - first guess for the data retained by the quality control.Cycle 90

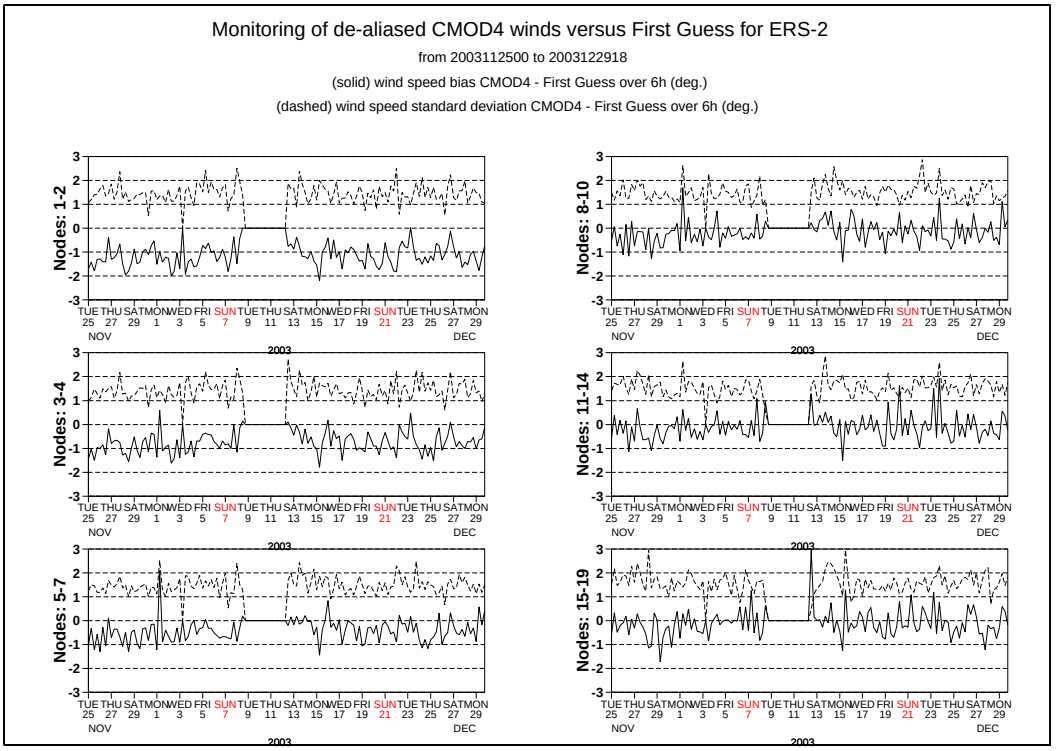

FIGURE 13. Same as Fig.12, but for the de-aliased CMOD-4 wind. Statistics are computed only for wind speeds higher than 4 m/s.Cycle 90

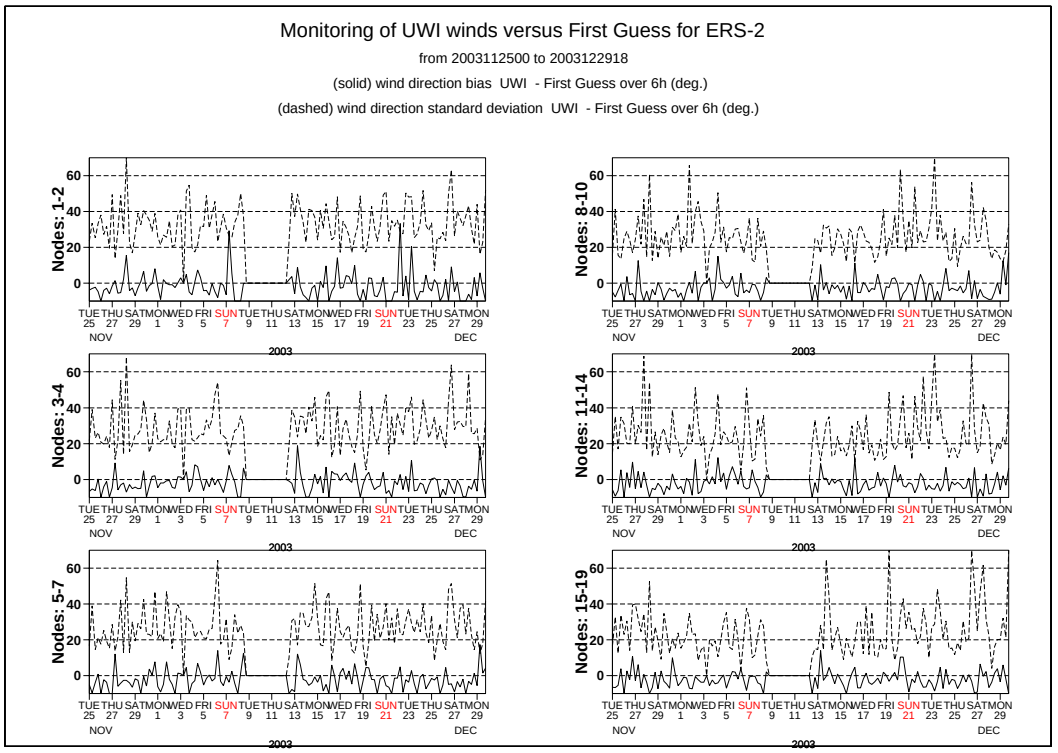

FIGURE 14. Same as Fig. 12 but for wind direction.Cycle 90.

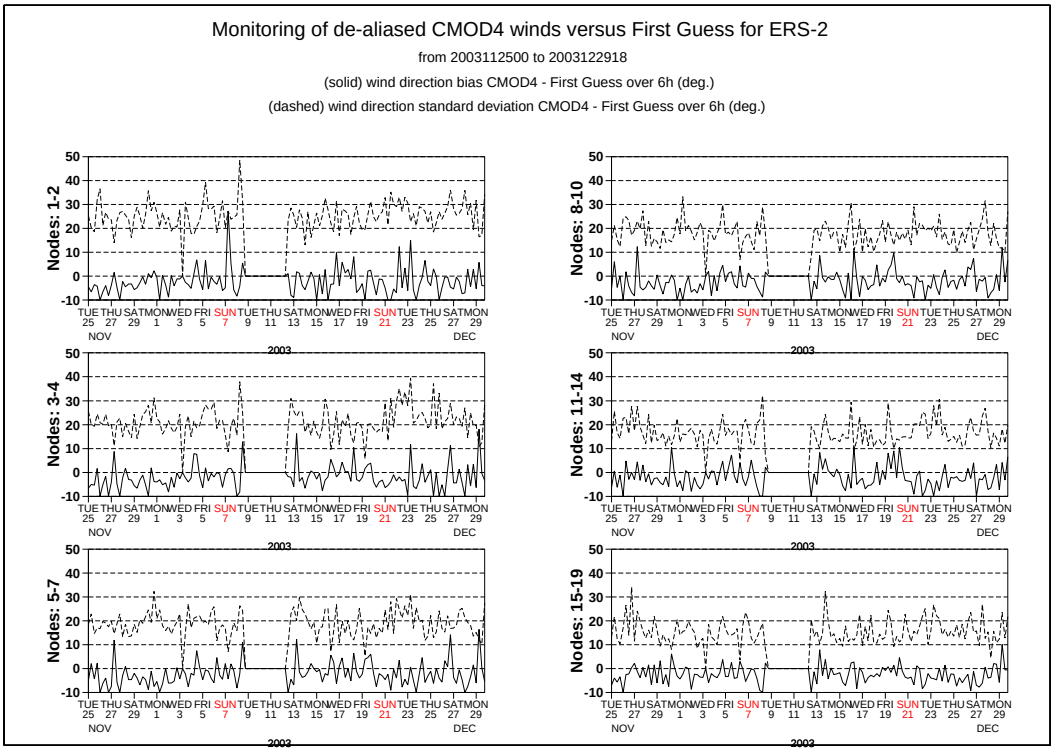

FIGURE 15. Same as Fig. 13 but for wind direction. Cycle 90.

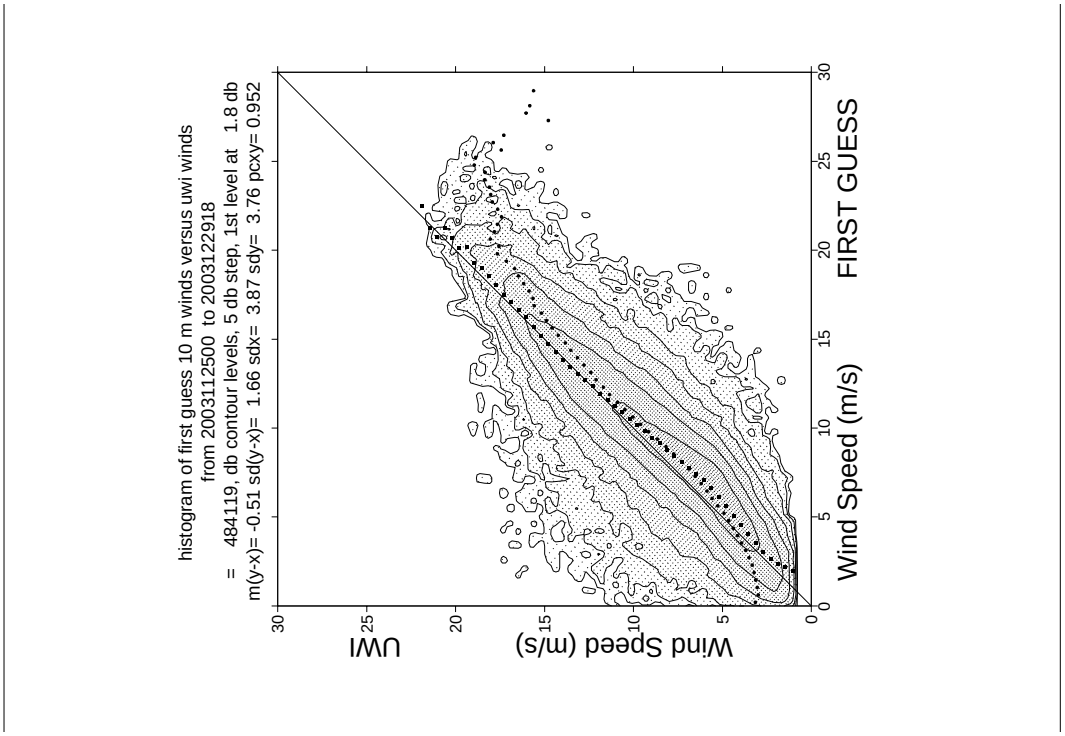

FIGURE 16. Two-dimensional histogram of first guess and UWI wind speeds, for the data kept by the quality control. Circles denote the mean values in the y-direction, and squares those in the x-direction.Cycle 90

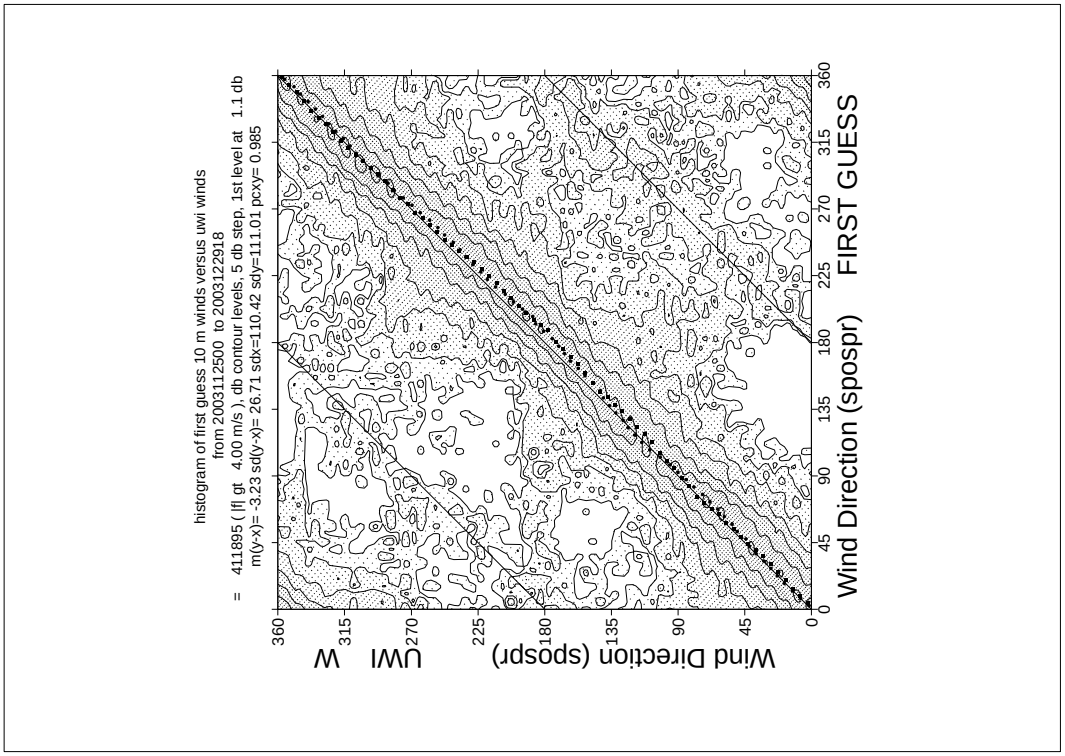

FIGURE 17. Same as Fig. 17, but for wind direction. Only wind speeds higher than 4m/s are taken into account. Cycle 90.

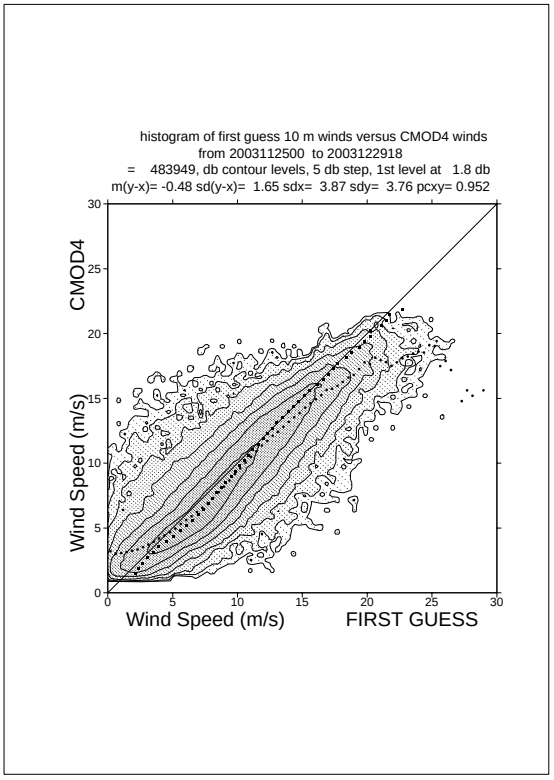

FIGURE 18. Same as Figure 16 but for de-aliased CMOD-4 winds. Cycle 90

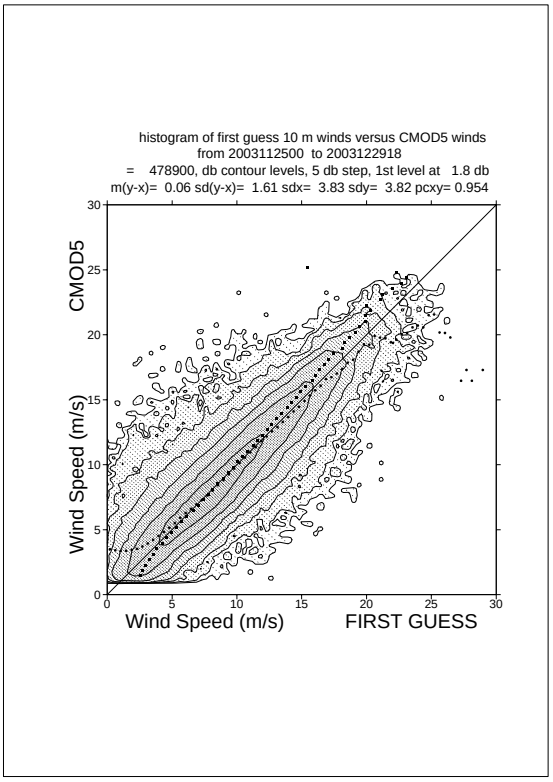

FIGURE 19. Same as Figure 16 but for de-aliased CMOD-5 winds. Cycle 90)

5.0 Yaw error angle estimation

The yaw error angle estimation is computed on-ground by the ESACA processors. The full set of results of the yaw processing is stored in an internal ESA product named HEY (Helpful ESA Yaw) disseminated from the ground station to ESRIN. The estimation of the yaw error angle is based on the Doppler shift measured on the received echo. That estimation can be done with a good accuracy only for small yaw error angle (in the range between +/- 4 deg.). Above that range, due to high Doppler frequency shift the signal spectrum is outside the receiver bandwidth and the yaw estimation is strong degraded. Details regarding the yaw processing can be found on the following document (chapter 9): http://earth.esa.int/pcs/ers/scatt/articles/soamain-030521.pdf

The yaw error angle estimation aims to compute the correct acquisition geometry for the three Scatterometer antenna throughout the entire orbit. The Yaw error angle information is used in the radar equation to derive the calibrated backscattering (sigma nought) from the Earth surface and to select the echo samples associated to one node. In ESACA the definition of the node position is as the one adopted in the old processor (for details see:.http://earth.esa.int/pcs/ers/scatt/articles/scatt_work98_processing.pdf). In such way the distance between the nodes (both along and across track) is kept constant (25 Km) and what is changing in function of the yaw error angle is the number of echo samples that contributes to the node calculation and the incidence angle of the measurement. This why the three scatterometer antennae could see the node with a different geometry due to an arbitrary variation of the yaw angle along track. The number of samples that actually contributes to a node and the yaw flag can be retrieved from the UWI Data Set Record (DSR) product. For that reason the definition of few fields in the UWI product has been updated.

The new definition of the fields number 8, 13 and 18 of the UWI DSR (see on page 50 in the ERS Ground Stations products Specification ER-IS-EPO-GS-0201) is as reported in Table 7

Table 7: New definition of field 8,13 and 18 in the UWI DSR

Field	Bytes	Type	old description	new description	Units
8	1	I1	counter of forebeam missing or corrupted source packets	counter of number of forebeam samples contributing to the node	1/8
13	1	I1	counter of midbeam missing or corrupted source packets	counter of number of midbeam samples contributing to the node	1/8
18	1	I1	counter of aftbeam missing or corrupted source packets	counter of number of aftbeam samples contributing to the node	1/8

The spare bit 15 and 16 had been used to store the yaw flag. The following definition updates the one on page 52 in the ERS Ground Stations products Specification ER-IS-EPO-GS-0201)

Table 8: New definition of bit 15 and bit 16 in the UWI DSR

Bit	0	1
Bit 15	Yaw error angle computed	Yaw error angle not computed due to strong degraded received spectrum or failure in the yaw retrieval algorithm

Table 8: New definition of bit 15 and bit 16 in the UWI DSR

Bit	0	1
Bit 16	Yaw within the threshold for the three beam Currently [-2,+2] degrees	Yaw above the threshold for any beam

For the BUFR users in order to maintain the compatibility with the actual decoder the following rules has been adopted in the encoding (UWI to BUFR format) processor in ESRIN and agreed during the 23rd ASCAT SAG:

- The BUFR field “number of missing source packet counter” (see ERS Products WMO FM94 BUFR Format ER-IS-UKM-GS-0001 Version 4 Issue 2 Table 5.15 Field 31) does not change its meaning
- The BUFR field “number of missing source packets counter” is filled with 0 if there are available more than 200 valid samples (120 in the Mid beam case) for the node or is filled with 32 (or -32 for wind/wave mode) if it is not the case.
- For the yaw angle flag, there is no spare room in the BUFR to add that information. To warn the user about a degradation of the data quality due to the yaw the rules in Table 9 has been defined to encode the BUFR PCD.

Table 9: Criteria to fill the BUFR DSR pcd

BUFR DSR pcd (Table 5.16)	Boolean Rule to set the pcd	New Meaning
Bit 2 No fore beam calculation	UWI pcd bit 2 oR UWI pcd bit 15	Fore beam not computed or Yaw angle not computed
Bit 3 No mid beam calculation	UWI pcd bit 3 oR UWI pcd bit 15	Mid beam not computed or Yaw angle not computed
Bit 4 No aft beam calculation	UWI pcd bit 4 oR UWI pcd bit 15	Aft beam not computed or Yaw angle not computed
Bit 7 Kp limit	UWI pcd bit 7 oR UWI pcd bit 16	Kp above the threshold or Yaw above the threshold

The figure 20 shows for each orbit the average doppler frequency shift (first 3 plots Fore Mid and Aft antenna), the minimum, maximum and mean yaw (fourth plot), the yaw standard deviation (fifth plot) and the percentage of source packets acquired with a yaw error angle outside the range +/- 2 degrees (sixth plot).

The result of the yaw monitoring for cycle 90 is a mean yaw error angle within the nominal range (+/- 2 degrees) for most of the orbit. On 25 and 26 November 2003 some orbits shows a bad quality due to a series of orbit manoeuvre.

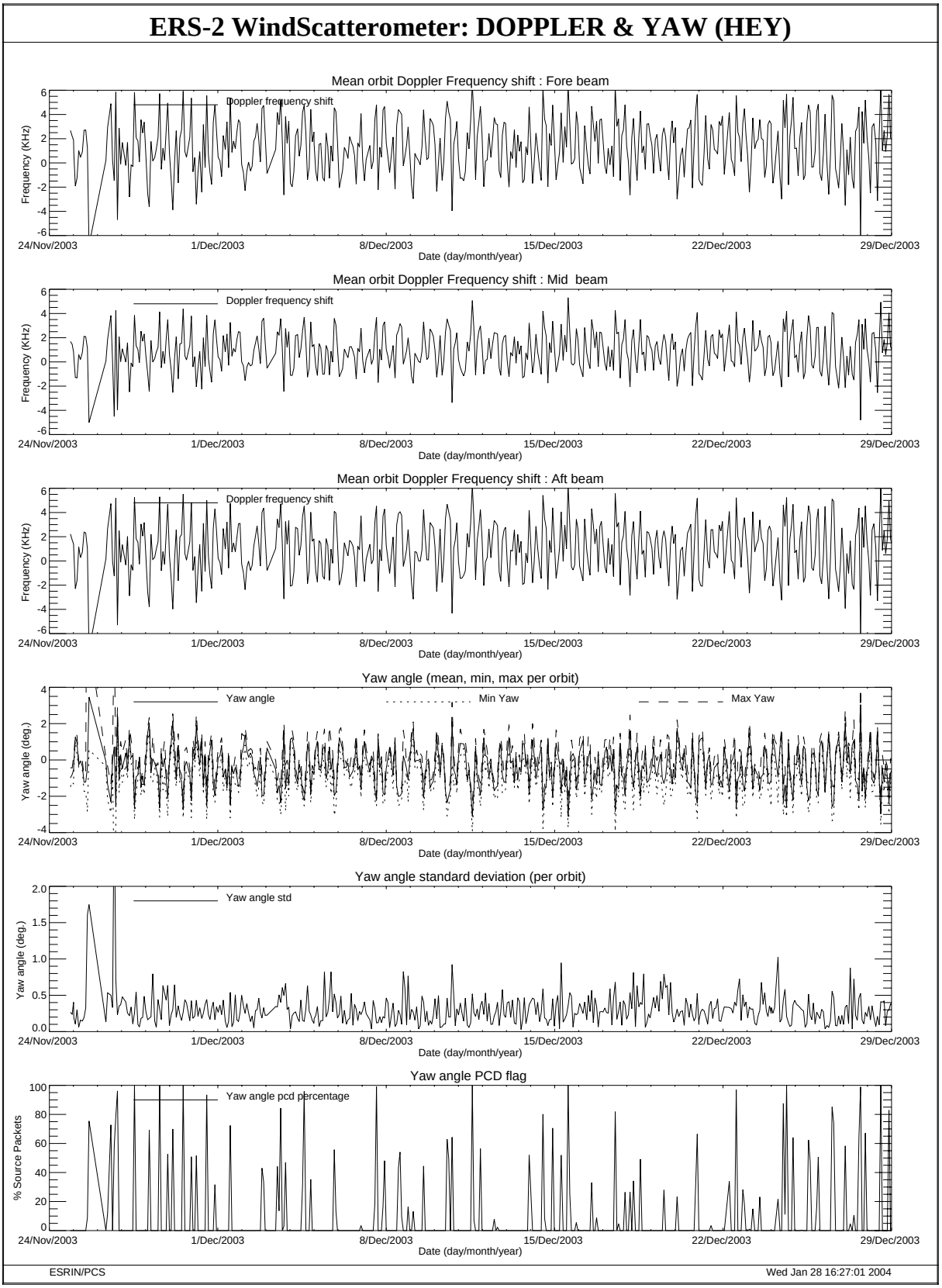

FIGURE 20. Doppler frequency shift and Yaw angle monitoring for cycle 90.